R. & M. No. 3685

R. & M. No. 3685

MINISTRY OF DEFENCE (PROCUREMENT EXECUTIVE)

AERONAUTICAL RESEARCH COUNCIL
REPORTS AND MEMORANDA

Vibration and Sound Generation in a Cascade of Flat Plates in Subsonic Flow

By

D. S. WHITEHEAD, M.A., Ph.D., M.I.Mech.E., A.F.R.Ae.S., C.Eng.
Cambridge University Engineering Department

LONDON: HER MAJESTY'S STATIONERY OFFICE
1972
PRICE £1·60 NET

Vibration and Sound Generation in a Cascade of Flat Plates in Subsonic Flow

By

D. S. WHITEHEAD, M.A., Ph.D., M.I.Mech.E., A.F.R.Ae.S., C.Eng.

Cambridge University Engineering Department

Reports and Memoranda No. 3685*
February, 1970

Summary.

The report gives particulars of a method of calculation, which has been programmed for a digital computer, for linearized two-dimensional subsonic unsteady flow through a cascade of flat plates operating at zero mean incidence. Inputs to the calculation are motion of the blades due to either bending or torsional vibration, wakes from moving obstructions upstream of the cascade, and incoming acoustic waves. For each of these inputs the output gives the force and moment on the blades, the wakes shed from the trailing edges, and the outgoing acoustic waves. The program therefore provides all the information necessary for calculation of forced and self-excited vibration of the blades, and for the generation, transmission, and reflection of acoustic waves by a cascade.

Two kinds of acoustic resonance are found, one corresponding to resonance of an annular duct without blades, and the other being an acoustic resonance in the passages between the blades.

Results are presented which illustrate the generation of acoustic waves by wakes. Results on torsional flutter indicate that compressibility has a very important effect. Whereas at low Mach number the worst position for the torsional axis is at about 75 per cent chord, as the Mach number is increased this position moves forward to the leading edge.

*Replaces A.R.C. 32 017.

LIST OF CONTENTS

1. *Introduction.*

This investigation is directed towards the elucidation of two of the most urgent problems which have arisen in the development of turbomachinery. These are blade vibration and generation of noise.

The blade vibration problem arises in two forms. First there is the question of what the amplitude will be due to forcing of say a rotor blade by stationary wakes and other forms of maldistribution in the inlet flow. Secondly there is the question of the conditions under which self-excited vibration or flutter can occur. In order to answer these questions it is necessary to know the forces and moments which act on the blade due to its vibratory motion and to the disturbances in the flow. These are now fairly well understood for two-dimensional unstalled incompressible flow, but practical blades usually operate at Mach numbers which are not small, so that the effect of compressibility is likely to be important. As soon as compressibility is introduced, the possibility of acoustic waves radiated by the blades arises, and these will be found to have a profound significance in the blade vibration problem.

In the noise generation problem it is recognized that there are a number of different ways in which turbomachinery blading can generate noise. Here, the relevant mechanisms are the generation of discrete tones due to wakes or other regular disturbances in the flow, and the generation of discrete tones due to blade vibration. Some indication will also be obtained of the generation of white noise due to turbulence in the inlet flow, but since this is really a three-dimensional problem, and the analysis to be given is two-dimensional, the application here is less direct. In addition the theory gives results for the way in which acoustic waves are reflected and transmitted by a cascade. Other mechanisms of noise generation such as the generation within turbulent boundary layers and wakes, and due to vortex shedding at trailing edges, are not relevant in the present context. This means that the results obtained will be of significance at the lower end of the noise frequency spectrum.

The assumptions made in the analysis are as follows:—

(a) The system considered is two-dimensional, so that the bending modes of actual blades are represented by a translational motion of the two-dimensional aerofoils, and the torsional modes of actual blades are represented by rotation of the two-dimensional aerofoils about a known axis. Only translational motion perpendicular to the chord line is considered.

(b) It is assumed that the blades do not stall, so that the flow always follows the blade surface.

(c) Effects due to camber and thickness are neglected, so that the blades are assumed to be flat plates.

(d) It is assumed that the blades operate at zero mean incidence, so that the mean deflection of the flow is zero, and that the Mach number of the mean flow is less than unity.

(e) The amplitude of the perturbations is assumed to be small. It follows that the wakes of the blades, which are vortex sheets in which the strength varies sinusoidally with distance from the trailing edge, can be taken to be straight. It also follows that the theory becomes linear, so that any two solutions for the perturbations can be superposed to give a third solution.

(f) It is assumed that events on all blades are identical, except for a constant phase change between each blade and the one above it. This involves no loss of generality, since any required solution can be built up by superposing solutions of the type considered.

(g) It is assumed that the fluid has zero viscosity, and that the Kutta-Joukowski condition at the trailing edges of the blades is satisfied.

Solutions of this problem have been given by Lane and Friedman[1], Gorolov and Dominas[2] and by Kaji and Okazaki[3]. The present work follows very closely the method due to Lane and Friedman, and the notation has been chosen to be largely identical with their report. Lane and Friedman, however, only computed the case of zero stagger with antiphase motion of the blades (corresponding to the wind tunnel wall interference problem) and did not consider the acoustic waves generated.

2. *Theory.*

2.1. *Basic Equations.*

The linearized equation for the pressure perturbation is

$$(1-M^2)\frac{\partial^2 p}{\partial x^2}+\frac{\partial^2 p}{\partial y^2}-\frac{2M}{c}\frac{\partial^2 p}{\partial x\,\partial t}-\frac{1}{c^2}\frac{\partial^2 p}{\partial t^2}=0\,.$$

For harmonic time dependence the pressure perturbation may be written

$$p=\bar{p}\exp(i\omega t)\,,$$

so that the basic differential equation becomes

$$(1-M^2)\frac{\partial^2 \bar{p}}{\partial x^2}+\frac{\partial^2 \bar{p}}{\partial y^2}-\frac{2i\omega M}{c}\frac{\partial \bar{p}}{\partial x}+\frac{\omega^2 \bar{p}}{c^2}=0\,.$$

It is convenient to solve this equation by making a Prandtl-Glauert transformation. Writing

$$\beta=\sqrt{(1-M^2)}$$

then the coordinates in the Prandtl-Glauert plane are

$$x'=x/\beta\,,$$

and

$$y'=y\,.$$

In this plane it is convenient to replace the pressure by the variable

$$\psi=\bar{p}\exp(-i\eta M x')\,. \tag{1}$$

The equation satisfied by ψ then becomes the reduced wave equation

$$\frac{\partial^2 \psi}{\partial x'^2}+\frac{\partial^2 \psi}{\partial y'^2}+\eta^2\psi=0\,,$$

where

$$\eta=\omega/c\beta\,.$$

The solution of this equation which is periodic in the x direction with wavenumber α is

$$\psi=f\exp\{i\alpha x'\pm i y'\sqrt{(\eta^2-\alpha^2)}\}\,. \tag{2}$$

The corresponding solution for the pressure is

$$p=f\exp\{i\omega t+i x(\alpha+\eta M)/\beta\pm i y\sqrt{(\eta^2-\alpha^2)}\}\,. \tag{3}$$

The velocity perturbations can be obtained from the linearized equations of motion,

$$\frac{\partial u}{\partial t}+U\frac{\partial u}{\partial x}=-\frac{1}{\rho}\frac{\partial p}{\partial x},$$

$$\frac{\partial v}{\partial t}+U\frac{\partial v}{\partial x}=-\frac{1}{\rho}\frac{\partial p}{\partial y},$$

giving

$$u=-\frac{f}{\rho U}\frac{\alpha+\eta M}{\alpha+\eta/M}\exp\{i\omega t+i x(\alpha+\eta M)/\beta\pm i y\sqrt{(\eta^2-\alpha^2)}\}, \tag{4}$$

and

$$v=\pm\frac{f\beta\sqrt{(\eta^2-\alpha^2)}}{\rho U}\frac{}{\alpha+\eta/M}\exp\{i\omega t+i x(\alpha+\eta M)/\beta\pm i y\sqrt{(\eta^2-\alpha^2)}\}. \tag{5}$$

The required solution for the cascade will be built up by superposing solutions of this type. But first it is necessary to consider the acoustic wave solutions which can exist far upstream and downstream of the cascade.

2.2. *Acoustic Wave Solutions.*

Since wavetype solutions can only exist when α is less than η, it is possible to write

$$\alpha=\eta\sin\lambda. \tag{6}$$

Then equation (2) becomes

$$\psi=f\exp\{i\eta(x'\sin\lambda-y'\cos\lambda)\}. \tag{7}$$

This represents a wave propagating in the Prandtl-Glauert plane at an angle λ measured anticlockwise from the y' axis. Four such waves are illustrated in Fig. 2, two propagating upstream and two downstream. These waves are shown diagramatically immediately upstream and downstream of the cascade, but of course close to the cascade there will be other effects due to the blades.

It is next necessary to determine what values of λ are consistent with the assumed phase angle σ between events on each blade and the one above it. At the origin, taken at the mid-chord of the reference blade,

$$\bar{p}=\psi=f.$$

At the mid-chord of the next blade above

$$x=s^*,\quad y=s,$$

and in the Prandtl-Glauert plane, where the blade spacing is d^*, and the stagger angle is ξ^*,

$$\begin{aligned} x'&=s^*/\beta=d^*\sin\xi^*,\\ \text{and}\qquad y'&=s\quad\ =d^*\cos\xi^*. \end{aligned} \tag{8}$$

Also on the next blade above

$$\bar{p} = f \exp(i\sigma),$$

so that from (1)

$$\psi = f \exp(i\sigma - i\eta Ms^*/\beta) = f \exp(i\Omega), \tag{9}$$

where

$$\Omega = \sigma - \eta Ms^*/\beta, \tag{10}$$

and is the phase angle change in ψ on going from one blade to the next in the Prandtl-Glauert plane.

From (7) and (8), on this blade

$$\begin{aligned}\psi &= f \exp\{i\eta(d^* \sin\xi^* \sin\lambda - d^* \cos\xi^* \cos\lambda)\} \\ &= f \exp\{-i\eta d^* \cos(\xi^* + \lambda)\}.\end{aligned} \tag{11}$$

Comparing (9) and (11) gives

$$\Omega = -\eta d^* \cos(\xi^* + \lambda) + 2\pi n,$$

where n is any integer.

If ζ is an angle defined by

$$\sin(\zeta) = (\Omega - 2\pi n)/\eta d^*, \quad (-\pi/2 < \zeta < \pi/2) \tag{12}$$

then

$$\cos(\xi^* + \lambda) = -\sin(\zeta)$$

and this is satisfied by two values of λ,

$$\begin{aligned}\lambda_1 &= \pi/2 + \zeta - \xi^*, \\ \text{and} \qquad \lambda_2 &= -\pi/2 - \zeta - \xi^*.\end{aligned} \tag{13}$$

These angles are illustrated in Fig. 2. ζ is the angle between the wavefronts (lines of constant ψ) and the cascade direction. It will be noted that $\lambda_1 > -\xi^*$, so that this always represents an upstream going wave and $\lambda_2 < -\xi^*$, so this always represents a downstream going wave. For the case illustrated in Figs. 1 and 2 there are two such wave pairs, corresponding to $n = 0$ and 1.

The corresponding picture in the physical plane is shown in Fig. 1. In a time of one period of the oscillation, one of the waves is convected from A to B at a velocity U, and is then propagated from B to C at a velocity c. The wavefronts (lines of constant p) are perpendicular to BC, and their inclination is given by the angle ϕ. It is found that

$$\begin{aligned}\sin\phi &= (M + \sin\lambda)/(1 + M \sin\lambda), \\ \text{and} \qquad \cos\phi &= \beta \cos\lambda/(1 + M \sin\lambda).\end{aligned} \tag{14}$$

Corresponding to equation (7) the pressure and velocity fluctuations are given by

$$\bar{p} = f \exp\{i\eta\beta(x\sin\phi - y\cos\phi)/(1 - M\sin\phi)\}, \tag{15}$$

$$\bar{u} = -(f/\rho c)\sin\phi \exp\{i\eta\beta(x\sin\phi - y\cos\phi)/(1 - M\sin\phi)\}, \tag{16}$$

and

$$\bar{v} = (f/\rho c)\cos\phi \exp\{i\eta\beta(x\sin\phi - y\cos\phi)/(1 - M\sin\phi)\}. \tag{17}$$

The concepts of acoustic wave-energy density and acoustic wave-energy flux in a moving medium have been discussed by Blokhintsev[4], Bretherton and Garrett[5], and Morfey[6]. Here the approach used by Bretherton and Garrett will be followed, and mean acoustic wave-energy density is defined in a frame of reference moving with the mean velocity of the fluid and is given by

$$E = \tfrac{1}{2}\rho < u^2 > + \tfrac{1}{2}\rho < v^2 > + \frac{1}{2\rho c^2} < p^2 > .$$

where the brackets $< >$ indicate time average values. The first two terms give the kinetic energy and the third term gives the potential energy. Substituting from equations (15), (16), and (17) and taking the average value gives

$$E = |f|^2/2\rho c^2 .$$

Bretherton and Garrett also show that the wave-energy flux is equal to the group velocity (c_j) times the wave-energy density. In this case the group velocity has components

$$c_x = U - c\sin\phi ,$$

and

$$c_y = c\cos\phi .$$

The wave energy flux is therefore given by

$$\dot{E}_x = c_x E = \frac{|f|^2}{2\rho c}(M - \sin\phi)$$

and

$$\dot{E}_y = c_y E = \frac{|f|^2}{2\rho c}\cos\phi .$$

The direction of energy propagation in the physical plane is given by the angle χ (measured anti-clockwise from the y axis) where

$$\tan\chi = -\frac{\dot{E}_x}{\dot{E}_y} = \frac{\sin\phi - M}{\cos\phi} = \beta\tan\lambda .$$

Hence the angle χ in the physical plane corresponds to the angle λ in the Prandtl-Glauert plane.

It is next necessary to recognize that acoustic wave energy is not conserved, since there can be energy exchange between the acoustic perturbations and the mean flow through the acoustic Reynolds stresses. However, Bretherton and Garrett show that under the approximations of geometrical acoustics a quantity called "total wave action" is conserved. If ω' is the intrinsic frequency, that is the frequency that would

be observed by an observer moving with the mean flow, then the quantity (E/ω') is the wave action density. It satisfies the conservation equation

$$\left(\frac{\partial}{\partial t}+c_j\frac{\partial}{\partial x_j}\right)\left(\frac{E}{\omega'}\right)+\left(\frac{\partial c_j}{\partial x_j}\right)\left(\frac{E}{\omega'}\right)=0\,.$$

This equation is true provided changes with time are small over one wave period and changes with distance are small over one wave length. The equation can also be written

$$\frac{\partial}{\partial t}\left(\frac{E}{\omega'}\right)+\frac{\partial}{\partial x_j}\left(\frac{c_j E}{\omega'}\right)=0\,.$$

In the application of these theoretical results to practical turbomachinery problems, the flow of acoustic power within the annulus of the machine is of less interest than the amount of acoustic power which emerges from the machine. It is therefore the latter quantity which will be calculated. It is supposed that the annulus in which the cascade is situated is fitted with a large contraction at inlet and a large diffuser at outlet, so that there are planes far upstream and downstream where the mean velocity is small. It is also supposed that the area variations are on a scale large compared to the wavelength of the sound so that the geometrical acoustics approximations can be applied within them. If the acoustic energy density is steady, then

$$\frac{\partial}{\partial t}\left(\frac{E}{\omega'}\right)=0\,.$$

Hence

$$\frac{\partial}{\partial x_j}\left(\frac{c_j E}{\omega'}\right)=0\,.$$

Applying the divergence theorem to the volume between a surface S_1 near the cascade and a surface S_2, where the mean velocity is low,

$$\int_{S_1}\left(\frac{n_j c_j E}{\omega'}\right)dS=\int_{S_2}\left(\frac{n_j c_j E}{\omega'}\right)dS\,,$$

where n_j is a unit vector normal to the surface, directed outwards from the machine.

On S_2 the velocity is low so that $\omega'=\omega$. Hence the acoustic power coming out is

$$W=\int_{S_2} n_j c_j E\,dS=\int_{S_1}(n_j c_j E\,\omega/\omega')\,dS\,.$$

The intrinsic frequency in the plane S_1 is found to be

$$\omega'=\omega/(1-M\sin\phi)\,.$$

So that if n_j is a unit vector in the axial direction

$$W=\{(U-c\sin\phi)\cos\xi-c\cos\phi\sin\xi\}\frac{|f|^2}{2\rho c^2}(1-M\sin\phi)\,S_1\,.$$

This may be written

$$W = \frac{|f|^2 \beta^2 S_1}{2\rho c} \frac{\cos\xi \cos\zeta \cos^2\phi}{\cos\xi^* \cos^2\lambda}. \tag{18}$$

The existence of pairs of acoustic waves is governed by equation (12), since the angle ζ only exists if

$$|\Omega - 2\pi n| < \eta d^*.$$

For given cascade geometry, phase angle, reduced frequency ($k = \omega b/U$), and integer n, the Mach number above which the wave pair exists is given by

$$\frac{1}{M^2} = 1 + 2\left(\frac{k\,d/b}{\sigma - 2\pi n}\right)\sin\xi + \left(\frac{k\,d/b}{\sigma - 2\pi n}\right)^2. \tag{19}$$

Alternatively, for given cascade geometry, phase angle, Mach number, and integer n, the reduced frequency above which the wave pair exists is given by

$$\frac{k\,d}{b} = \frac{(\sigma - 2\pi n)\beta\cos\xi^*}{M\cos\xi\,(M\sin\xi^* \pm 1)}. \tag{20}$$

At the point of appearance of the acoustic waves the angle ζ is $\pm 90°$, so that the direction of energy propagation is along the cascade, and no energy is removed by the waves from the vicinity of the cascade. This gives a resonance condition, and also corresponds to the cut-off condition discussed by Tyler and Soffrin[7].

2.2. *Cascade Solution.*

The cascade solution will now be built up from the basic solutions given by equations (3), (4) and (5). Initially the case when there is only one blade in the plane $y = 0$ will be considered.

The choice of the sign ambiguity in these equations may be made from physical considerations. If α is less than η then the solutions are wave-type and only waves propagating away from the blade are admissible. If α is greater than η then the solutions are exponential with y and only those solutions which remain finite as y becomes large and positive or negative are admissible. In both cases this means that the lower sign must be taken in the upper half plane and the upper sign must be taken in the lower half plane.

An alternative way of making this choice, which is more powerful mathematically, is to assume that ω, η and k all have a small negative imaginary part.

$$\omega = \omega_1 + i\,\omega_2,$$
$$\eta = \eta_1 + i\,\eta_2,$$
$$k = k_1 + i\,k_2,$$

where ω_2, η_2 and k_2 are all small and negative. This gives

$$p = \bar{p}\exp(i\,\omega_1 t - \omega_2 t)$$

This corresponds to a slightly divergent oscillation. Waves originating at large distances from the cascade, which were emitted at much earlier times, are therefore small. Also, the strength of the vortex sheet in the wakes of the blades becomes small far downstream, since the vorticity is convected at the

mainstream velocity U and was therefore shed at much earlier times. Then

$$\sqrt{(\eta^2-\alpha^2)} = \sqrt{(\eta_1^2-\alpha^2)}+i\,\eta_1\,\eta_2/\sqrt{(\eta_1^2-\alpha^2)}$$

to first order in η_2. Hence, for the wave-type solution

$$\exp\{\pm i\,y\sqrt{(\eta^2-\alpha^2)}\} = \exp\{\pm i\,y\sqrt{(\eta_1^2-\alpha^2)}\mp\eta_1\,\eta_2\,y/\sqrt{(\eta_1^2-\alpha^2)}\}.$$

In order to have a solution which decays far away from the blades, it is necessary, since η_2 is negative, to take the lower sign in the upper half plane and the upper sign in the lower half plane. This is the same condition as before.

The solutions in the two half planes are matched so that they give the same velocity perturbation v in the y direction in the plane $y = 0$. The complete solution for a single blade is then obtained by integrating the basic solutions for all possible values of α. The result is

$$p = \tfrac{1}{2}\,sgn(y)\int_{-\infty}^{+\infty} f_0(\alpha)\exp\{i\omega t+ix(\alpha+\eta M)/\beta-i|y|\sqrt{(\eta^2-\alpha^2)}\}\,d\alpha, \tag{21}$$

$$u = -\frac{1}{2\rho U}\,sgn(y)\int_{-\infty}^{+\infty} f_0(\alpha)\frac{\alpha+\eta M}{\alpha+\eta/M}\exp\{i\omega t+ix(\alpha+\eta M)/\beta-i|y|\sqrt{(\eta^2-\alpha^2)}\}\,d\alpha \tag{22}$$

and

$$v = \frac{\beta}{2\rho U}\int_{-\infty}^{+\infty} f_0(\alpha)\frac{\sqrt{(\eta^2-\alpha^2)}}{\alpha+\eta/M}\exp\{i\omega t+ix(\alpha+\eta M)/\beta-i|y|\sqrt{(\eta^2-\alpha^2)}\}\,d\alpha. \tag{23}$$

The amplitude of the pressure jump across the $y = 0$ plane (pressure just above the plane minus pressure just below the plane) is then given by

$$[\bar{p}] = \int_{-\infty}^{+\infty} f_0(\alpha)\exp\{ix(\alpha+\eta M)/\beta\}\,d\alpha. \tag{24}$$

This shows that $[\bar{p}]$ is the Fourier transform of the function f_0, except for the effect of the ηM term which merely shifts the effective origin of α. The form of $f_0(\alpha)$ will have to be adjusted to make $[\bar{p}]$ zero off the blade.

The corresponding jump in u velocity is

$$[\bar{u}] = -\frac{1}{\rho U}\int_{-\infty}^{+\infty} f_0(\alpha)\frac{\alpha+\eta M}{\alpha+\eta/M}\exp\{ix(\alpha+\eta M)/\beta\}\,d\alpha. \tag{25}$$

The solution for the m^{th} blade can be obtained from equations (21), (22) and (23) by writing x_m for x, y_m for y and f_m for f_0, where

$$x_m = x - m\,s^*\,,$$

$$y_m = y - m\,s\,,$$

$$f_m = f_0 \exp(i\,m\,\sigma)\,,$$

since on the m^{th} blade, pressures and velocities are advanced in phase by an angle $m\sigma$. Summing the effects of all blades gives for the amplitude of the upwash velocity

$$\bar{v} = \frac{\beta}{2\,\rho\,U}\int_{-\infty}^{+\infty} f_0(\alpha)\frac{\sqrt{(\eta^2-\alpha^2)}}{\alpha+\eta/M}\times\sum_{m=-\infty}^{m=+\infty}\exp\{\,ix_m(\alpha+\eta M)/\beta - i|y_m|\sqrt{(\eta^2-\alpha^2)} + im\sigma\,\}\,d\alpha\,. \tag{26}$$

The series in this expression is a geometric progression and can be summed. The small negative imagary part of $\sqrt{(\eta^2-\alpha^2)}$ is used to obtain convergence. Then for the range $0 \leqslant y \leqslant s$ the result is

$$\bar{v} = \frac{\beta}{2\,\rho\,U}\int_{-\infty}^{+\infty} f_0(\alpha)\frac{\sqrt{(\eta^2-\alpha^2)}}{\alpha+\eta/M}\exp\{\,ix\,(\alpha+\eta M)/\beta\,\}\times$$

$$\left[\frac{\exp\{\,i(y-s)\sqrt{(\eta^2-\alpha^2)} - is^*\,(\alpha+\eta M)/\beta + i\sigma\,\}}{1-\exp\{\,-is\sqrt{(\eta^2-\alpha^2)} - is^*\,(\alpha+\eta M)/\beta + i\sigma\,\}} + \right.$$

$$\left. + \frac{\exp\{\,-iy\sqrt{(\eta^2-\alpha^2)}\,\}}{1-\exp\{\,-is\sqrt{(\eta^2-\alpha^2)} + is^*\,(\alpha+\eta M)/\beta - i\sigma\,\}}\right] d\alpha\,. \tag{27}$$

It will be convenient to write these expressions in non-dimensional form. The quantities η, α and f_0 are replaced by μ, τ, and F_0, where

$$\eta = \mu\,\beta/b\,, \tag{28}$$

$$\alpha = \tau\,\beta/b\,, \tag{29}$$

and

$$f_0(\alpha) = F_0(\tau)\,\rho\,b\,U^2/\beta\,. \tag{30}$$

Then the pressure jump across the blade is given by

$$\left[\frac{\bar{p}}{\rho\,U^2}\right] = \int_{-\infty}^{+\infty} F_0(\tau)\exp\{\,ix\,(\tau+\mu\,M)/b\,\}\,d\tau\,. \tag{31}$$

The jump in u velocity across the blade is given by

$$\left[\frac{\bar{u}}{U}\right] = -\int_{-\infty}^{+\infty} F_0(\tau)\frac{\tau+\mu M}{\tau+\mu/M}\exp\{\,ix\,(\tau+\mu M)/b\,\}\,d\tau\,. \tag{32}$$

The upwash velocity is, for $y=0$

$$\frac{\bar{v}}{U} = \frac{\beta}{2}\int_{-\infty}^{+\infty} F_0(\tau)\frac{\sqrt{(\mu^2-\tau^2)}}{\tau+\mu/M}\exp\{ix(\tau+\mu M)/b\}\times \tag{33}$$

$$\left[\frac{\exp\{-is\beta\sqrt{(\mu^2-\tau^2)}/b - i\tau s^*/b + i\Omega\}}{1-\exp\{-is\beta\sqrt{(\mu^2-\tau^2)}/b - i\tau s^*/b + i\Omega\}} + \frac{1}{1-\exp\{-is\beta\sqrt{(\mu^2-\tau^2)}/b + i\tau s^*/b - i\Omega\}}\right] d\tau$$

$$= -\frac{i\beta}{2}\int_{-\infty}^{+\infty} F_0(\tau)\frac{\sqrt{(\mu^2-\tau^2)}}{\tau+\mu/M}\frac{\exp\{ix(\tau+\mu M)/b\}\sin\{s\beta\sqrt{(\mu^2-\tau^2)}/b\}}{\cos(\Omega-\tau s^*/b)-\cos\{s\beta\sqrt{(\mu^2-\tau^2)}/b\}}\,d\tau\,. \tag{34}$$

2.3. *Upwash Velocities.*

The form of the function $F_0(\tau)$ is initially unknown, and has to be determined to give the required upwash velocities on the surface of the blade. In this report five different kinds of upwash velocities are considered.

First, due to bending motion of the blade the upwash velocity is $q\exp(i\omega t)$. This gives

$$\frac{\bar{v}}{q} = 1\,. \tag{35}$$

Secondly, due to torsional motion of the blade about an axis at the mid chord through an angle $\theta\exp(i\omega t)$ (anticlockwise positive) the velocity normal to the chord line is

$$(\bar{v}-\theta U)\exp(i\omega t) = x\frac{d}{dt}\left\{\theta\exp(i\omega t)\right\}.$$

This gives

$$\frac{\bar{v}}{U\theta} = 1 + i\,k\,x/b\,. \tag{36}$$

The third type of upwash velocity is that which would be generated by wakes from some kind of periodic obstruction far upstream of the cascade under consideration. It is supposed that a Fourier analysis of the wake profile has been carried out, and one component is considered. The wake spacing and the relative velocity of motion of the obstructions determine the frequency ω and the phase angle σ of the disturbance felt by the cascade. It will be supposed that the upwash velocity which the disturbance would induce at the origin (at the mid-point of the reference blade) if the cascade were removed is $w_o\exp(i\omega t)$. Then since the whole disturbance is convected downstream at a velocity U, the upwash velocity at any point (x, o) is

$$w_o\exp(i\omega t - i\omega x/U)\,.$$

There is no pressure perturbation associated with this flow.

Since the total induced upwash velocity must be zero, this is equal and opposite to the velocity induced by the pressure jump across the blades, $\bar{v}\exp(i\omega t)$. Hence

$$\bar{v} = -w_o\exp(-i\omega x/U) = -w_o\exp(-i\,k\,x/b)\,. \tag{37}$$

The fourth type of upwash velocity is due to acoustic waves propagating in an upstream direction from some other source further downstream. The upwash velocity is of the form given by equation (5), with the value of α given by $\eta \sin \lambda_1$. This may be written

$$\begin{aligned} \bar{v} &= -w_1 \exp \{ i x \eta (M + \sin \lambda_1)/\beta \}, \\ &= -w_1 \exp \{ i \mu (M + \sin \lambda_1) x/b \}. \end{aligned} \tag{38}$$

Similarly the fifth type of upwash velocity is due to acoustic waves propagating in a downstream direction from some other source upstream. The upwash velocity expression is

$$\bar{v} = -w_2 \exp \{ i \mu (M + \sin \lambda_2) x/b \}. \tag{39}$$

2.4. *Lift and Moment.*

Equation (31) may be interpreted as showing that $[\bar{p}/\rho U^2] \exp(-ix\mu M/b)$ is the Fourier transform of $F_o(\tau)$. The transform may therefore be inverted to give

$$F_o(\tau) = \frac{1}{2\pi} \int_{-\infty}^{+\infty} \left[\frac{\bar{p}}{\rho U^2} \right] \exp \{ -i x (\tau + \mu M)/b \} \, d(x/b). \tag{40}$$

Since $[\bar{p}]$ is zero off the blade the limits may be replaced by $-b$ to $+b$. Then putting $\tau = -\mu M$ gives

$$\begin{aligned} F_o(-\mu M) &= \frac{1}{2\pi} \int_{-b}^{+b} \left[\frac{\bar{p}}{\rho U^2} \right] d(x/b), \\ &= -\frac{\bar{L}}{2 \pi \rho U^2 b}, \end{aligned} \tag{41}$$

where $\bar{L}$ is the amplitude of the aerodynamic lift acting on the blade.

If equation (40) is differentiated with respect to τ and then τ is put equal to $-\mu M$,

$$\begin{aligned} F_0'(-\mu M) &= \frac{1}{2\pi} \int_{-b}^{+b} \left[\frac{\bar{p}}{\rho U^2} \right] (-i x/b) \, d(x/b), \\ &= -\frac{i \bar{M}_o}{2 \pi \rho U^2 b^2}, \end{aligned} \tag{42}$$

where $\bar{M}_o$ is the amplitude of the aerodynamic moment (positive nose up) about the mid-chord point.

2.5. *Strength of the Shed Vortex Sheet.*

The strength of the vortex sheet which replaces the reference blade and its wake is given by equation (32). It is now required to find the strength of the sheet far downstream when $x \to +\infty$.

It will be found that the equation for the upwash velocity can be satisfied by taking for $F_o(\tau)$ an expansion in terms of Bessel functions. These Bessel functions contain no singularity on the x axis. Thus the integral in equation (32) contains just one singularity at the point $\tau = -\mu/M$. This singularity may be separated out as follows,

$$\left[\frac{\bar{u}}{U}\right] = \int_{-\infty}^{+\infty} \left\{\frac{D}{\tau+\mu/M} + E(\tau)\right\} \exp\left\{i\, x(\tau+\mu M)/b\right\} d\tau\,.$$

Here $E(\tau)$ is without singularity and D is given by

$$D = F_o(-\mu/M)\frac{\mu\,\beta^2}{M} = k\,F_o(-k/\beta^2)\,.$$

When $|x| \to \infty$ the $E(\tau)$ term does not contribute anything. The contribution of the D term may be evaluated by Jordan's Lemma. This states that if $Q(z) = N(z)/D(z)$, where $N(z)$ and $D(z)$ are polynomials, $D(z)$ has no real roots, and the degree of $D(z)$ exceeds the degree of $N(z)$ by at least one, then if $z > 0$

$$\int_{-\infty}^{+\infty} Q(\tau)\exp(i\,\tau\,z)\,d\tau = 2\pi i\,\Sigma\,R^{+}\,,$$

and

$$\int_{-\infty}^{+\infty} Q(\tau)\exp(-i\,\tau\,z)\,d\tau = -2\pi i\,\Sigma\,R^{-}\,,$$

where $\Sigma\,R^{+}$ and $\Sigma\,R^{-}$ denote the residues of $Q(z)\exp(i\,\tau\,z)$ and $Q(z)\exp(-i\,\tau\,z)$ in the upper and lower half planes respectively. In this case

$$\mu = \mu_1 + i\,\mu_2$$

where μ_2 is small and negative. The pole is therefore just in the upper half plane.

Hence if $x \to -\infty$

$$\left[\frac{\bar{u}}{U}\right] = 0\,,$$

and if $x \to +\infty$

$$\left[\frac{\bar{u}}{U}\right] \to \quad 2\,\pi\,i\,D\exp(-i\,\mu\,x\,\beta^2/M\,b)$$

$$= 2\,\pi\,i\,k\,F_o(-k/\beta^2)\exp(-i\,k\,x/b)\,.$$

The amplitude of the vortex sheet far downstream is therefore given by

$$\frac{\varepsilon}{U} = -2\,\pi\,i\,k\,F_0(-k/\beta^2)\,. \tag{43}$$

2.6. *Strength of Acoustic Waves Far Upstream and Downstream.*

The acoustic waves far upstream and downstream radiated from the cascade can be obtained in a similar way from an examination of the singularities occurring in equations (33) and (34). There is one singularity occurring at $\tau = -\mu/M$. There may also be other singularities occurring when

$$-s\beta\sqrt{(\mu^2-\tau^2)}/b-\tau s^*/b+\Omega = +2\pi n,$$

or

$$-s\beta\sqrt{(\mu^2-\tau^2)}/b+\tau s^*/b-\Omega = -2\pi n,$$

where n is an integer. The values of τ which satisfy these equations are

$$\tau_1 = \mu \sin \lambda_1$$

and

$$\tau_2 = \mu \sin \lambda_2$$

where λ_1 and λ_2 are given by equations (13). The singularities in the integral therefore correspond exactly to the possible acoustic waves far upstream and downstream.

In the following the equations will be written as if just one pair of acoustic waves can exist, but the terms for further pairs of acoustic waves can be added in exactly the same form.

Equation (34) for the upwash velocity on $y = 0$ can therefore be written in the form

$$\frac{\bar{v}}{U} = \int_{-\infty}^{+\infty} \left\{ \frac{B}{\tau-\tau_1} + \frac{C}{\tau-\tau_2} + \frac{D}{\tau+\mu/M} + E(\tau) \right\} \exp\{ i x(\tau+\mu M)/b \}\, d\tau, \tag{44}$$

where $E(\tau)$ is without singularity and the constants B, C, and D are given by

$$B = \frac{i\mu b}{2d^*} \frac{F_o(\tau_1)}{(\tau_1+\mu/M)} \frac{\cos^2\lambda_1}{\cos\zeta},$$

$$C = -\frac{i\mu b}{2d^*} \frac{F_o(\tau_2)}{(\tau_2+\mu/M)} \frac{\cos^2\lambda_2}{\cos\zeta},$$

$$D = \frac{ik}{2} F_o(-k/\beta^2) \frac{\sinh(ks/b)}{\cos(\Omega+ks^*/\beta^2 b)-\cosh(ks/b)}$$

When $|x|\to\infty$ the $E(\tau)$ term does not contribute anything, and the other terms may be evaluated by Jordan's Lemma as before. It is found that τ_1, has a small negative imaginary part so that τ_1, is just in the lower half plane, and similarly τ_2 is just in the upper half plane. Also, the pole at $\tau = -\mu/M$ is just in the upper half plane.

Hence if $x\to-\infty$,

$$\frac{\bar{v}}{U} = -2\pi i B \exp\{ ix(\tau_1+\mu M)/b \}.$$

This shows the acoustic wave propagating upstream, the amplitude of the upwash velocity being

$$\frac{\bar{v}_1}{U} = -2\pi i B = +\frac{\pi b M}{d^*} \frac{F_o(\mu \sin\lambda_1)}{(M\sin\lambda_1+1)} \frac{\cos^2\lambda_1}{\cos\zeta}. \tag{45}$$

Also if $x\to+\infty$,

$$\frac{\bar{v}}{U} = +2\pi i C \exp\{ ix(\tau_2+\mu M)/b \} + 2\pi i D \exp(-ikx/b).$$

This shows an acoustic wave propagating downstream and the velocity associated with the shed vortex sheets, which are convected downstream at the mainstream velocity U. The amplitude of the upwash velocity in the acoustic wave going downstream is

$$\frac{\bar{v}_2}{U} = 2\pi i\, C = \frac{\pi\, b\, M}{d^*} \frac{F_o(\mu \sin \lambda_2)}{(M \sin \lambda_2 + 1)} \frac{\cos^2 \lambda_2}{\cos \zeta}. \tag{46}$$

The amplitude of the pressure fluctuations associated with these waves can be obtained from equations (15) and (17). The pressure fluctuation in the upstream going wave is

$$\frac{\bar{p}}{\rho\, U^2} = -\frac{\pi\, b}{\beta\, d^*} \frac{\cos \lambda_1}{\cos \zeta} F_o(\mu \sin \lambda_1). \tag{47}$$

with a similar expression for the downstream going wave.

It is interesting to note that the required output quantities, lift, moment, shed vortex sheet, and radiated acoustic waves, are all determined by certain specific points on the $F_o(\tau)$ function. The moment depends on the slope of the function, and all the other quantities are given by the ordinate at the relevant point. This situation is illustrated in Fig. 3.

It is also interesting to note what happens when $\mu \to 0$. Since $\mu = \omega b/c\beta^2$, this occurs when the wavelength of sound is much greater than the blade chord. Then both the lift and the amplitude of the acoustic waves radiated depend on $F_o(0)$, and the relationship between the pressure fluctuation in the upstream going wave and the lift is

$$\frac{\bar{p}}{\rho\, U^2} = \frac{\bar{L}}{2\rho\, U^2\, \beta\, d^*} \frac{\cos \lambda_1}{\cos \zeta} \tag{48}$$

This is a form of the well known relationship between lift and radiated sound waves, and can be shown to be identical with equations (27) in a paper by Mani[8].

The corresponding power per unit annulus-area radiated outside the machine is, from equation (18),

$$W = \frac{\bar{L}^2\, S_1 \cos^2 \phi \cos \xi^*}{8\rho\, d^2 c \cos \zeta \cos \xi}. \tag{49}$$

This can be shown to be identical to Mani's equations (28). It should be noted, however, that it only applies to the acoustic power coming from a stationary cascade. If the cascade is moving then the work done by the mean flow on the acoustic wave packet on its way out of the machine will be altered, and the result will be different.

2.7. *Expansion in Series.*

It is next assumed that the pressure difference across the blade can be expressed as a trigonometrical series, in the usual manner of thin aerofoil theory;

$$\left[\frac{\bar{p}}{\rho\, U^2}\right] = \tfrac{1}{2} A_o \cot(\gamma/2) \pm \sum_{r=1}^{\infty} A_r \sin r\gamma,$$

where $x/b = -\cos \gamma$.*

This assumption automatically satisfies the Kutta-Joukowski condition at the trailing edges of the blades, where the pressure difference is zero.

---

*Note that the A_o used here is double the A_o used in Lane and Friedman's paper.

Substituting this into equation (40) and evaluating the integrals gives

$$F_o(\tau) = \tfrac{1}{4} A_o \{ J_o(\tau+\mu M) + i J_1(\tau+\mu M) \} +$$

$$+ \sum_{r=1}^{\infty} \tfrac{1}{4} i^{r-1} A_r \{ J_{r-1}(\tau+\mu M) + J_{r+1}(\tau+\mu M) \}, \tag{50}$$

where the J's indicate the usual Bessel functions.

Putting $\tau = -\mu M$ and using equation (41) gives for the lift force

$$\frac{\bar{L}}{\rho U^2 b} = -\frac{\pi}{2}(A_o + A_1). \tag{51}$$

Differentiating equation (50) with respect to τ, putting $\tau = -\mu M$, and using equation (42) gives for the moment

$$\frac{\bar{M}_0}{\rho U^2 b^2} = -\frac{\pi}{4}(A_o + A_2). \tag{52}$$

These two output quantities therefore depend on only the first three A_r coefficients, but the other output quantities depend on the whole series of A_r coefficients.

2.8. *Evaluation of the Upwash Integral.*

In determining the A_r coefficients, it will be assumed that the $F_o(\tau)$ function is sufficiently characterised by taking the first n_a of them. These n_a coefficients are then determined by making the upwash velocity at n_a points along the chord match the required upwash velocities. It is therefore necessary to evaluate the upwash velocities from equation (34), when $F_o(\tau)$ is given by each of the functions in equation (50) by which the A_r coefficients are multiplied. These are

$$F_{oo}(\tau) = \tfrac{1}{4} \{ J_o(\tau+\mu M) + i J_1(\tau+\mu M) \}, \tag{53}$$

$$F_{or}(\tau) = \tfrac{1}{4} i^{r-1} \{ J_{r-1}(\tau+\mu M) + J_{r+1}(\tau+\mu M) \}$$

$$= \tfrac{1}{2} i^{r-1} \frac{r}{\tau+\mu M} J_r(\tau+\mu M), r > 0. \tag{54}$$

The integrals have to be evaluated numerically. Two difficulties arise. The first is that the integrand contains singularities, which have to be subtracted out and evaluated analytically. The second difficulty is the behaviour at large values of τ, since the integrand oscillates with amplitude proportional to $|\tau|^{-1/2}$, indicating slow convergence and requiring special numerical techniques.

The singularities will be subtracted out, not in the way used in equation (44), but with the exponential terms included in the coefficients.

$$\frac{\bar{v}}{U} = \int_{-\infty}^{+\infty} \left[-\frac{i\beta}{2} F_{or}(\tau) \frac{\sqrt{(\mu^2-\tau^2)}}{\tau+k/\beta^2} \frac{\exp\{ix(\tau+\mu M)/b\} \sin\{s\beta\sqrt{(\mu^2-\tau^2)}/b\}}{\cos(\Omega-\tau s^*/b)-\cos\{s\beta\sqrt{(\mu^2-\tau^2)}/b\}} - \right.$$

$$\left. -\frac{B'}{\tau-\tau_1} - \frac{C'}{\tau-\tau_2} - \frac{D'}{\tau+k/\beta^2} \right] d\tau + \int_{-\infty}^{-\infty} \left[\frac{B'}{\tau-\tau_1} + \frac{C'}{\tau-\tau_2} + \frac{D'}{\tau+k/\beta^2} \right] d\tau .$$

Here

$$B' = B \exp\{ ix(\tau_1+\mu M)/b \},$$
$$C' = C \exp\{ ix(\tau_2+\mu M)/b \},$$
$$D' = D \exp\{ -ikx/b \}.$$

Since τ_1 is just in the lower half plane

$$\int_{-\infty}^{+\infty} \frac{B'}{\tau-\tau_1} d\tau = -i\pi B' .$$

Also since τ_2 and $(-k/\beta^2)$ are just in the upper half plane,

$$\int_{-\infty}^{+\infty} \frac{C'}{\tau-\tau_2} d\tau = +i\pi C',$$

and

$$\int_{-\infty}^{+\infty} \frac{D'}{\tau+k/\beta^2} d\tau = +i\pi D' .$$

It is then convenient to divide the integral into three ranges. First there is the inner range $-\mu < \tau < +\mu$. In this range it is convenient to make the substitution

$$\tau = \mu \sin\lambda .$$

Also in this range the subtraction of the singularity at $\tau = -\mu/M$ is unnecessary, and this can be evaluated analytically

$$-\int_{-\mu}^{+\mu} \frac{D'}{\tau+\mu/M} d\tau = -D' \log \frac{1+M}{1-M} .$$

The second range includes both $-\tau_s < \tau < -\mu$ and $\mu < \tau < +\tau_s$, where τ_s is chosen to be large enough to make the special methods used for the infinite integral accurate, and is certainly greater than μ/M. In this range the subtraction of the singularities at τ_1 and τ_2 is unnecessary, and these can be evaluated analytically.

$$\left[\int_{-\tau_s}^{-\mu} + \int_{+\mu}^{+\tau_s}\right]\left[-\frac{B'}{\tau-\tau_1} - \frac{C'}{\tau-\tau_2}\right] d\tau$$

$$= -B' \log \frac{(\mu+\tau_1)(\tau_s-\tau_1)}{(\tau_s+\tau_1)(\mu-\tau_1)} - C' \log \frac{(\mu+\tau_2)(\tau_s-\tau_2)}{(\tau_s+\tau_2)(\mu-\tau_2)}.$$

The third range includes both $\tau < -\tau_s$ and $\tau > \tau_s$. In this range all the singularity terms can be evaluated analytically.

$$\left[\int_{-\infty}^{-\tau_s} + \int_{\tau_s}^{+\infty}\right]\left[-\frac{B'}{(\tau-\tau_1)} - \frac{C'}{(\tau-\tau_2)} - \frac{D'}{(\tau+\mu/M)}\right] d\tau$$

$$= -B' \log \frac{\tau_s+\tau_1}{\tau_s-\tau_1} - C' \log \frac{\tau_s+\tau_2}{\tau_s-\tau_2} - D' \log \frac{\tau_s-\mu/M}{\tau_s+\mu/M}.$$

The complete expression for the upwash velocity is then

$$\frac{\bar{v}}{U} = \int_{-\pi/2}^{+\pi/2} \left[\frac{i\beta\mu M \cos\lambda}{2(M\sin\lambda+1)} \frac{F_{or}(\mu\sin\lambda)\exp\{i\mu x(\sin\lambda+M)/b\}\sin\{s\beta\mu\cos\lambda/b\}}{\cos\{s\beta\mu\cos\lambda/b\} - \cos\{\Omega-\mu s^*\sin\lambda/b\}} - \right.$$

$$\left. - \frac{B'}{\sin\lambda-\sin\lambda_1} - \frac{C'}{\sin\lambda-\sin\lambda_2}\right] \cos\lambda\, d\lambda +$$

$$+ \left[\int_{-\tau_s}^{-\mu} + \int_{+\mu}^{+\tau_s}\right]\left[\frac{-i\beta\sqrt{(\tau^2-\mu^2)}}{2(\tau+k/\beta^2)} \frac{F_{or}(\tau)\exp\{ix(\tau+\mu M)/b\}\sinh\{s\beta\sqrt{(\mu^2-\tau^2)}/b\}}{\cosh\{s\beta\sqrt{(\mu^2-\tau^2)}/b\} - \cos\{\Omega-\tau s^*/b\}} - \right.$$

$$\left. - \frac{D'}{\tau+k/\beta^2}\right] d\tau +$$

$$+ \left[\int_{-\infty}^{-\tau_s} + \int_{+\tau_s}^{+\infty}\right]\left[\frac{-i\beta\sqrt{(\tau^2-\mu^2)}}{2(\tau+k/\beta^2)} \frac{F_{or}(\tau)\exp\{ix(\tau+\mu M)/b\}\sinh\{s\beta\sqrt{(\mu^2-\tau^2)}/b\}}{\cosh\{s\beta\sqrt{(\mu^2-\tau^2)}/b\} - \cos\{\Omega-\tau s^*/b\}}\right] d\tau +$$

$$+ B'\left\{\log\frac{1-\sin\lambda_1}{1+\sin\lambda_1} - i\pi\right\} + C'\left\{\log\frac{1-\sin\lambda_2}{1+\sin\lambda_2} + i\pi\right\} + D'\left\{\log\frac{(\tau_s+k/\beta^2)(1-M)}{(\tau_s-k/\beta^2)(1+M)} + i\pi\right\}. \qquad (55)$$

The first two integrals in this expression can be evaluated by numerical quadrature. A Gaussian 5-point formula is used, and is applied over each strip between the ends of the range, the points $\lambda = \pm\xi^*$, and the singularities. This is satisfactory except when the Mach number is just below that at which a pair of acoustic waves appears. Then the integrand grows a large peak at the point where the corresponding singularities are about to appear, at $\lambda = \pm\xi^*$, and the quadrature becomes slightly less accurate.

Similar methods are used for the second range, except that the maximum width of strip used for the application of a Gauss 5-point formula is 1·0.

2.9. *Evaluation of Infinite Integral.*

In evaluating the integrals with infinite limits in equation (55) it is first noted then if τ is sufficiently large, the factor

$$\frac{\sinh\{s\beta\sqrt{(\tau^2-\mu^2)}/b\}}{\cosh\{s\beta\sqrt{(\tau^2-\mu^2)}/b\}-\cos\{\Omega-\tau s^*/b\}}$$

is nearly unity. If τ_s is chosen so that

$$s\beta\sqrt{(\tau_s^2-\mu^2)}/b=11{\cdot}5\,,$$

then the maximum error is 0·00002.

This simplifies the integral, and also means that it becomes independent of the cascade geometry and the phasing between blades. If, therefore, calculations with a number of different phase angles are required, then the infinite integral can be pre-tabulated and used in each case. The integral is the same as that which would occur with an isolated aerofoil.

Since the integral is slowly convergent, Euler's transformation, Ref. 9, will be used for its evaluation. However, this transformation only applies if the integrand is a periodic function with slowly decreasing amplitude, and the period must be known. Some rearrangement is necessary in order to put the integral in the required form.

Since the argument is large, the Bessel functions in equations (53) and (54) may be evaluated by the asymptotic series

$$J_r(z)=\sqrt{\left(\frac{2}{\pi z}\right)}\left\{P_r\cos(z-r\pi/2-\pi/4)-Q_r\sin(z-r\pi/2-\pi/4)\right\},$$

where

$$P_r(z)=1-\frac{(4r^2-1)(4r^2-9)}{2!(8z)^2}+\ldots$$

and

$$Q_r(z)=\frac{(4r^2-1)}{(8z)}-\frac{(4r^2-1)(4r^2-9)(4r^2-25)}{3!(8z)^3}+\ldots$$

After some manipulation the integral for $r=0$ may be written as

$$\int_{\tau_s}^{\infty}\frac{\beta}{\tau+k/\beta^2}\left\{\frac{(\tau^2-\mu^2)}{128\,\pi(\tau+\mu M)}\right\}^{\frac{1}{2}}$$

$$\left[\left\{-i\,P_o(\tau+\mu M)+Q_o(\tau+\mu M)-i\,P_1(\tau+\mu M)+Q_1(\tau+\mu M)\right\}\exp i\left\{(\tau+\mu M)(1+x/b)-\pi/4\right\}+\right.$$

$$\left.+\left\{-i\,P_o(\tau+\mu M)-Q_o(\tau+\mu M)+i\,P_1(\tau+\mu M)+Q_1(\tau+\mu M)\right\}\exp-i\left\{(\tau+\mu M)(1-x/b)-\pi/4\right\}\right]d\tau+$$

$$+\int_{\tau_s}^{\infty}\frac{\beta}{-\tau+k/\beta^2}\left\{\frac{(\tau^2-\mu^2)}{128\,\pi(\tau-\mu M)}\right\}^{\frac{1}{2}}$$

$$\left[\left\{-i\,P_o(\tau-\mu M)-Q_o(\tau-\mu M)-i\,P_1(\tau-\mu M)-Q_1(\tau-\mu M)\right\}\exp-i\left\{(\tau-\mu M)(1+x/b)-\pi/4\right\}+\right.$$

$$+\left\{-i\,P_o(\tau-\mu M)+Q_o(\tau-\mu M)+i\,P_1(\tau-\mu M)-Q_1(\tau-\mu M)\right\}\exp i\left\{(\tau-\mu M)(1-x/b)-\pi/4\right\}\Big]d\tau\,. \tag{56}$$

Similarly the integral for $r>0$ may be written as

$$\int_{\tau_s}^{\infty}\frac{2r\beta}{(\tau+k/\beta^2)(\tau+\mu M)}\left\{\frac{(\tau^2-\mu^2}{128\,\pi\,(\tau+\mu M)}\right\}^{\frac{1}{2}}$$

$$\Big[\left\{-P_r(\tau+\mu M)-i\,Q_r(\tau+\mu M)\right\}\exp i\left\{(\tau+\mu M)(1+x/b)-\pi/4\right\}+$$

$$+\left\{-P_r(\tau+\mu M)+i\,Q_r(\tau+\mu M)\right\}\exp -i\left\{(\tau+\mu M)(1-x/b)-\pi/4-r\pi\right\}\Big]d\tau+$$

$$+\int_{\tau_s}^{\infty}\frac{2r\beta}{(-\tau+k/\beta^2)(\tau-\mu M)}\left\{\frac{(\tau^2-\mu^2)}{128\,\pi\,(\tau+\mu M)}\right\}^{\frac{1}{2}}$$

$$\Big[\left\{P_r(\tau-\mu M)-i\,Q_r(\tau-\mu M)\right\}\exp -i\left\{(\tau-\mu M)(1+x/b)-\pi/4\right\}$$

$$+\left\{P_r(\tau-\mu M)+i\,Q_r(\tau-\mu M)\right\}\exp i\left\{(\tau-\mu M)(1-x/b)-\pi/4-r\,\pi\right\}\Big]d\tau\,. \tag{57}$$

In each integral the integrand is periodic with a period of either $2\pi/(1+x/b)$ or $2\pi/(1-x/b)$. All the other terms in the integral are slowly varying. The integrals may therefore be evaluated by applying Euler's transformation twice, once for each of these periods.

In the choice of τ_s it is necessary to ensure that

$$\tau_s > 6+r^2/10+\mu M\,,$$

in order to ensure an accuracy of 10^{-5} in the asymptotic series P_r and Q_r, and also

$$\tau_s > 3\,k/\beta^2\,,$$

in order to keep well clear of the singularity at $\tau=-k/\beta^2$.

2.10. *Matrix Form of the Equations.*

In order to determine the first n_a of the A_r coefficients, it is necessary to match the upwash velocity at n_a points along the chords of the aerofoils. In choosing these points it is necessary to avoid the ends of the aerofoil, $x=\pm b$, since equations (56) and (57) show that the period of the integrand becomes infinite for these points, and the Euler transformation no longer works. The points are therefore chosen so that

$$\frac{x_j}{b}=\frac{2j}{n_a+1}-1\,,\quad 1\leqslant j\leqslant n_a\,. \tag{58}$$

The required upwash velocities at these points are given by equations (35), (36), (37), (38) and (39), for the five different types of input disturbance. If all five types of disturbance are present together, then the total upwash velocity may be written as follows

$$\bar{v} = [1, (1+i\,k\,x_j/b), \exp(-i\,k\,x_j/b), \exp\{i\,\mu\,(M+\sin\lambda_1)\,x_j/b\}, \exp\{i\,\mu\,(M+\sin\lambda_2)\,x_j/b\}]$$

$$\times \begin{bmatrix} q \\ U\,\theta \\ -w_0 \\ -w_1 \\ -w_2 \end{bmatrix}$$

$$= \mathbf{V}\,\mathbf{U}, \tag{59}$$

where **V** and **U** are the matrices shown. The equations are written for the case when there is just one wave pair. If there were n_w wave pairs, then **V** would have n_a rows and $3+2n_w$ columns, and **U** would have $3+2n_w$ rows. The choice of signs in these matrices, and the dimensionalizing factor U in **U**, has been made to make the resulting coefficients consistent with those used in Ref. 10.

The upwash velocities induced by the A_r coefficients may be written as follows

$$\frac{\bar{v}}{U} = \mathbf{B}\,\mathbf{A}\,. \tag{60}$$

Here the matrix **B** (which is n_a by n_a) has elements b_{jr}, where b_{jr} is the velocity induced at x_j by the coefficient of A_r, and **A** is a column matrix of the A_r coefficients with n_a rows. b_{jr} is obtained from equations (55), (56), and (57).

Equating the upwash velocities given by equations (59) and (60), and solving for the unknown matrix **A** gives

$$\mathbf{A} = \left(\frac{1}{U}\right)\mathbf{B}^{-1}\,\mathbf{V}\,\mathbf{U}\,. \tag{61}$$

The required results are obtained from equations (51), (52), (43), (45) and (46), and may be written in the form

$$\begin{bmatrix} \bar{L}\,2\pi\rho\,b\,U \\ -\bar{M}_o/4\,\pi\,\rho\,b^2\,U \\ \varepsilon \\ \bar{v}_1 \\ \\ \bar{v}_2 \end{bmatrix} = U \begin{bmatrix} -\frac{1}{4} & -\frac{1}{4} & 0 & 0 & . & . \\ +\frac{1}{16} & 0 & +\frac{1}{16} & 0 & . & . \\ \left\{-2\pi\,i\,k \quad F_{or}(-k/\beta^2)\right\} & & & & & \\ \left\{\frac{\pi\,b\,M}{d^*}\,\frac{F_{or}(\mu\sin\lambda_1)}{1+M\sin\lambda_1}\,\frac{\cos^2\lambda_1}{\cos\zeta}\right\} & & & & & \\ \left\{\frac{\pi\,b\,M}{d^*}\,\frac{F_{or}(\mu\sin\lambda_2)}{1+M\sin\lambda_2}\,\frac{\cos^2\lambda_2}{\cos\zeta}\right\} & & & & & \end{bmatrix} \begin{bmatrix} A_0 \\ A_1 \\ A_2 \\ \\ \\ \\ \end{bmatrix}$$

$$= U\,\mathbf{D}\,\mathbf{A}\,. \tag{62}$$

Here **D** is a matrix with $3+2n_w$ rows and n_a columns.

Eliminating the matrix **A** between equations (61) and (62), the final result may be written in the form

$$\begin{bmatrix} \bar{L}/2\pi\rho b U \\ -\bar{M}/4\pi\rho b^2 U \\ \varepsilon \\ \bar{v}_1 \\ \bar{v}_2 \end{bmatrix} = \mathbf{C} \begin{bmatrix} q \\ U\theta \\ -w_0 \\ -w_1 \\ -w_2 \end{bmatrix}, \tag{63}$$

where $\mathbf{C} = \mathbf{D}\,\mathbf{B}^{-1}\,\mathbf{V}$. (64)

The matrix **C** is the principal output from the computer program, and is obtained from equation (64). Equation (63) shows how these results are to be interpreted. **C** is square and has $3+2n_w$ rows and columns.

Elements in the first two rows and first three columns correspond to the coefficients C_{Fq}, $C_{F\alpha}$, C_{Fw}, C_{Mq}, $C_{M\alpha}$ and C_{Mw} used in Ref. 10, but they are referred to an axis position at the mid-chord point instead of the axis position at the leading edge used in that Report.

3. *Computer Program.*

A computer program to carry out the calculation has been written in ASA Fortran. The program was initially developed on a small IBM 1130 computer, but it was found to be too big to be convenient on this machine, since it was necessary to divide the program into three sections and to call them up from the disc store into the core store in turn for execution. This gives long running times. The program was therefore transferred to TITAN, a much larger computer in the Cambridge University Mathematical Laboratory. On TITAN the time to compute each point is approximately $4n_a^2$ seconds. The programme requires 16 K of core store. The present programme is limited to two wave pairs and to a maximum n_a of 7.

4. *Results.*

In this report no extensive or systematic investigation of any particular effect has been carried out, since this would require a large amount of computer time. Instead, some comparisons with previous work have been carried out, in order to check the correctness of the program, and some specific examples which illustrate important points have been computed.

4.1. *Comparison with Incompressible Results.*

The comparison with some incompressible results taken from Ref. 10 is shown in Table 1. These results have been referred to an axis position at the leading edge of the blade.

It is seen that there is good agreement between the two sets of results. The greatest discrepancy is 0·0180, which occurs with the high stagger angle of 75 degrees. These results were taken with the upwash velocities matched at four points ($n_a = 4$), and the accuracy could be improved at the expense of longer computing times by taking larger values of n_a. However, $n_a = 4$ appears to give an accuracy which is quite sufficient for engineering purposes, and this value has been used for all subsequent results except for the comparison in the next two sections.

4.2. *Comparison with Lane and Friedman.*

The comparison with some of Lane and Friedman's results[1] is shown in Table 2.

For this cascade geometry and phase angle, the frequency parameter at which waves appear (from equation (20)) is 1·4320. The comparison between the two sets of results shows good agreement at all frequency parameters, but the agreement is slightly less good at a frequency parameter of 1·4. This illustrates the previous statement that the numerical integration techniques which have been used become slightly inaccurate at frequency parameters or Mach numbers just below those at which a pair of acoustic waves appears.

4.3. *Comparison with Kaji and Okazaki.*

Kaji and Okazaki[3] have given results for the case of an upstream going wave approaching the cascade from downstream. Their results in one particular cascade are shown in Fig. 4, and four points, *A*, *B*, *C*, and *D* calculated by the present program (with $n_a = 3$) have been superposed. The full line shows the amplitude of the transmitted wave and the dashed line shows the amplitude of the reflected wave. At *A* the incident wave front is normal to the mainstream flow, and the wave goes through with no reflection. At *B* the phase angle (σ) is zero. At *C* the reflected wave front is normal to the mainstream flow, the downstream going wave does not interact with the cascade, and the amplitude of the reflected wave is zero. At *D*, which is very close to cut-off conditions, there is almost total reflection of the incident wave with no transmission.

These four points all show good agreement between Kaji and Okazaki's results and the present programme.

4.4. *Example of Wave Generation at Low Mach Number.*

Fig. 5 shows results which have been obtained for comparison with a current experiment. A rotor with 23 blades is to be run in an airstream with 24 obstructions at inlet, which produces wakes which interact with the rotor blades. The cut-off condition occurs at a Mach number of 0·0867, and above this one wave pair can exist. The amplitude of the pressure fluctuations in the generated waves going upstream and downstream is shown. The amplitude is very large just above the cut-off condition and decreases rapidly. The amplitude of the downstream wave becomes zero at a Mach number of 0·2. At this point the wavefronts in the downstream going wave are normal to the mainstream flow, and this wave does not interact with the cascade. It may be of practical interest to note that if the number of rotor blades was one more rather than one less than the number of obstructions, then it would be the upstream wave strength which would go through a zero.

Fig. 5 also shows the magnitude of the lift fluctuation on the blades due to the same wakes. The lift rises just below the cut-off condition. Immediately above the cut-off condition the lift is zero, but it rapidly rises to a value not very different from the incompressible result. This is of significance in connection with the traditional method of calculating noise generation, which is to use an incompressible theory to calculate the lift fluctuation, and then use this in a purely acoustic calculation, equivalent to equation (48), to get the sound waves produced. Fig. 5 shows that this will give good estimates except for the region just above the cut-off condition where the results are quite wrong.

Fig. 5 also shows the acoustic power radiated from the machine, calculated on the assumption that the blades are stationary, so that the obstructions would have to be rotating, using equation (18). The important point is that the acoustic power just above cut-off is quite finite, although the associated pressure fluctuations are infinite. This is because the energy is propagating in a mainly tangential direction, so that the axial energy flow does not become large.

4.5. *Example of Wave Generation at High Mach Number.*

Fig. 6 shows an example of wave generation in which the first pair of acoustic waves appears at a Mach number of 0·7998, and the second pair of acoustic waves appears at a Mach number of 0·959. There is therefore only a comparatively narrow range of Mach number over which there is just one wave pair, but within this range the behaviour of the acoustic waves and the lift fluctuation is similar to the previous example. There is however a difference in the behaviour of the lift force just below the cut-off point, since in the high Mach number example the force appears to be tending to zero at the cut-off point, whereas in the low Mach number example the force appears to be increasing as the cut-off point is approached.

4.6. *Comparison with Parker's Resonance Condition.*

In Ref. 11, Parker has calculated the frequency of acoustic resonances in a cascade of flat plates at zero stagger, when there is no mean flow through the cascade. This corresponds to a special case of the present theory, when the frequency parameter tends to infinity, the Mach number tends to zero,

but the product of these two quantities remains finite. Comparison of the two theories should therefore be possible.

The present program cannot be run at very high frequency parameters for several reasons. Some of these reasons are fairly trivial, and arise from the use of U as a non-dimensionalizing factor. More fundamental difficulties arise owing to the singularity at $\tau = -k/\beta^2$ occurring at large negative values of τ, and because the upwash velocity shows very rapid fluctuations along the chord, so that very large values of n_a would be required to represent it properly. However, the program has been run at a frequency parameter of 10, and the results are shown in Fig. 7.

This figure shows the real and imaginary parts of the blade force coefficient, due to bending motion of the blades. This represents a convenient way to excite the acoustic resonance. The Mach number for cut-off is 0·1975, and the Mach number at which resonance is predicted from Parker's[11] calculations is 0·172. The resonance appears very clearly. The real part of the force coefficient shows a large negative peak, and the imaginary part shows a zero with negative and positive peaks close either side of it.

This is exactly the behaviour to be expected from forced vibration of a single-degree-of-freedom damped oscillator. At the resonant peak a large aerodynamic force is obtained from a small movement of the blade. The position of the resonance does not quite agree with Parker's calculation: this is probably due to the steady flow at a Mach number of about 0·16 modifying the acoustic resonant frequency of the system. However, the general prediction of the effect is excellent.

4.7. *Bending Vibration.*

Bending flutter of blades is controlled by the real part of the coefficient C_{Fq}. If this is positive the aerodynamic forces do work on the vibration, and if there is no mechanical damping, bending flutter occurs. No case of bending flutter has been found from the present program. Although no systematic search has been carried out to look for this effect, it seems likely that it does not occur under the present assumption of zero incidence. It is known that for incompressible flow, bending flutter depends on steady loading of the blades[12]. It therefore appears that there would not be much significance in looking for bending flutter until steady lift can be included in the compressible theory.

As a by-product of runs carried out for other purposes, information has been obtained on the amplitude of bending vibration forced at resonance by wakes from obstructions upstream, assuming that there is no mechanical damping. Some of this is shown on Fig. 8, where the resonance factor given by

$$|q/w_0| = -|C_{Fw}|/\mathscr{R}(C_{Fq})$$

is plotted against Mach number for two cases.

Since the lift force on the blades tends to zero at the cutoff condition for the acoustic waves, and therefore the aerodynamic damping disappears, it might be thought that the forced vibration would be very great at this point. This is not so because the aerodynamic exciting forces also tend to zero, and the resonance factors shown in Fig. 8 tend to finite limits just above the cut-off condition. In fact in the low Mach number case it looks as though the forced vibration tends to zero at this point.

The behaviour just below the cut-off point is different in the two cases. In the high Mach number case the forced vibration becomes large, but in the low Mach number case it becomes small.

4.8. *Torsional Flutter.*

If there is no mechanical damping, then it is shown in Ref. 13 that the marginal condition for torsional flutter is

$$\mathscr{I}(C_{M\alpha})_x = 0,$$

where the coefficient $(C_M)_x$ is referred to an axis position x corresponding to the position of the node in the first torsional mode of the blades. The imaginary part of this coefficient does work on the vibration, and if it is positive then flutter can occur.

This coefficient is related to the coefficients referred to the mid-chord point by the equation

$$(C_{M\alpha})_x = C_{M\alpha} - \left(\frac{x}{2b}\right) C_{F\alpha} - i(2k)\left(\frac{x}{2b}\right) C_{Mq} + i(2k)\left(\frac{x}{2b}\right)^2 C_{Fq}.$$

The condition for marginal torsional flutter is therefore

$$\mathscr{I}(C_{M\alpha}) - \left(\frac{x}{2b}\right)\mathscr{I}(C_{F\alpha}) - (2k)\left(\frac{x}{2b}\right)\mathscr{R}(C_{Mq}) + (2k)\left(\frac{x}{2b}\right)^2 \mathscr{R}(C_{Fq}) = 0.$$

For given cascade geometry, Mach number, frequency parameter and phase angle, this equation may be regarded as a quadratic for $(x/2b)$ which may or may not have real roots. The program has been arranged to find the real roots, if there are any. Some results are shown on Fig. 9, where the values of $(x/2b)$ are plotted against phase angle.

These critical axis positions form loops, and inside the loops the imaginary part of $(C_{M\alpha})_x$ is positive so that flutter can occur. Since flutter can occur at any phase angle to suit itself, it is the extreme values of axis position for each loop which are of main interest.

The cascade shown in Fig. 8 has a geometry fairly typical of a trans-sonic tip section, but the frequency parameter is only about one third of what would be allowed in practice so that severe flutter occurs. At the lower Mach numbers the region of instability is centred around an axis position at about 75 per cent chord, but as the Mach number increases the axis positions move forward, and at 0·8 the centre of the region is located forward of the leading edge.

5. *Conclusions.*

The method of solution proposed by Lane and Friedman has been found to be capable of extension to calculate acoustic waves and the vorticity shed from the trailing edge, and to accept inputs of acoustic waves and vorticity shed from upstream obstructions. The method leads to a computer program which provides all the data necessary to predict the generation, transmission and reflection of acoustic waves by a cascade, the behaviour of blades in bending and torsional vibration, and the interactions between the acoustic waves and the vibration. The accuracy achieved is more than sufficient for engineering purposes, but the amount of computer time needed is fairly substantial.

It has been found that two different types of acoustic resonance are important. The first is an acoustic resonance of an annular duct without blades and corresponds to the cut-off condition for transmission of waves down the duct. At this condition the blades can vibrate with no aerodynamic force on them. The second type of acoustic resonance is one which may occur within the cascade, and is the type calculated by Parker. The effect of a uniform velocity through the cascade is to introduce damping of the resonance. At this resonance, in the limit of no flow, the blades can have a finite aerodynamic force on them with no blade motion or any other type of forcing.

The results for the generation of acoustic waves by wakes entering the cascade from some other moving obstruction upstream show that the waves appear suddenly, as the Mach number is raised, at the cut-off condition with very large amplitude of pressure fluctuations. However, these waves are travelling very nearly in the tangential direction, and the amount of acoustic power which emerges from the machine is finite. If the blade chord is much less than the acoustic wavelength, then there is a simple relationship between the blade force and the strength of the acoustic waves generated. This is the basis of the traditional method of calculating the wave generation, and it is usual to use an incompressible theory to obtain the force fluctuations. The results obtained here show that the traditional approach will give reasonably accurate answers provided that conditions are not close to the cut-off condition. But as cut-off is approached the traditional approach predicts infinite acoustic power generation, whereas the more accurate approach used here shows finite acoustic power.

No case of pure bending flutter has been found, but it has been found that compressibility has a major effect on torsional flutter. Whereas incompressible theory predicted that a torsional axis position at

75 per cent chord is very bad for torsional flutter, it is found that at high subsonic Mach numbers the worst axis position tends to move forward along the chord. This matter appears to be of considerable practical importance, and further investigation is clearly required.

Acknowledgement.

Grateful acknowledgement is made to Prof. M. V. Wilkes, who made the computing facilities at the Cambridge University Mathematical Laboratory available to the author, and also to the Ministry of Technology, who supported the work.

LIST OF SYMBOLS

Some of the notation used is illustrated in Figs. 1 and 2.

A_r	Coefficients in pressure jump expansion.
B, B'	Strength of singularity associated with upstream going acoustic wave.
C, C'	Strength of singularity associated with downstream going acoustic wave.
D, D'	Strength of singularity associated with shed vortex sheet.
E	Acoustic wave energy density.
$\dot{E}$	Acoustic wave energy flux.
$E(\tau)$	Function of τ without singularity.
F_o	$= \beta f_o/\rho b U^2$. Non-dimensional form of f_o.
F_{or}	Coefficient of A_r in expansion of F_o.
J_r	Bessel functions.
L	Aerodynamic force per unit span.
M	Mach number.
M_x	Aerodynamic moment, positive nose up, about point $(x, 0)$ per unit span.
P, Q	Asymptotic series for Bessel function evaluation.
S_1	Annulus area.
S_2	Area of control surface outside machine.
U	Mainstream velocity.
W	Acoustic power output.
b	Blade semi-chord.
c	Speed of sound.
d	Blade spacing.
d^*	Blade spacing in Prandtl-Glauert plane.
f	Amplitude of pressure fluctuation.
f_m	Amplitude of pressure-jump solution for m^{th} blade.
i	$= \sqrt{(-1)}$. Indicates component leading 90 degrees in phase.
j	Integer specifying matching point along chord.
k	$= \omega b/U$. Reduced frequency. ($2k$ = Frequency parameter).
m	Integer specifying number of blade.
n	Integer specifying phase angle for acoustic waves.
n_a	Number of points taken in numerical approximation.
n_w	Number of wave pairs.
p	Pressure.

q	Blade velocity due to vibration.
r	Integer specifying number of A_r coefficient.
s	Gap distance, measured normal to chord.
s^*	Stagger distance, measured parallel to chord.
t	Time.
u, v	Velocity perturbations.
w_o	Amplitude of perturbation velocity due to incident wakes.
w_1, w_2	Amplitude of perturbation velocities due to incident acoustic waves.
x, y	Coordinates parallel and normal to chord lines.
x', y'	Coordinates in Prandtl-Glauert plane.
α	Wave-number in x' direction in Prandtl-Glauert plane.
β	$= \sqrt{(1-M^2)}$.
γ	$\cos\gamma = -x/b$. Substitution for x.
ε	Amplitude of vortex sheet shed from trailing edge.
ζ	Angle between waves and cascade in Prandtl-Glauert plane.
η	$= \omega/c\beta$.
θ	Torsional displacement of blade.
λ	Propagation direction in Prandtl-Glauert plane.
λ_1, λ_2	Values of λ for upstream and downstream going waves.
μ	$= b\eta/\beta = \omega b/c\beta^2$. Non-dimensional form of η.
ξ	Stagger angle.
ξ^*	Stagger angle in Prandtl-Glauert plane.
ρ	Density.
σ	Interblade phase angle.
τ	$= b\alpha/\beta$. Non-dimensional form of α.
ϕ	Wave angle in physical plane.
χ	Direction of energy propagation in physical plane.
ψ	Modified pressure for Prandtl-Glauert plane.
ω	Angular frequency.
ω'	Intrinsic frequency.
Ω	Interblade phase angle in Prandtl-Glauert plane.

Matrices

A	$n_a \times (3+2n_w)$	Columns of A_r coefficients.
B	$n_a \times n_a$	Induced velocity matrix.
C	$(3+2n_w) \times (3+2n_w)$	Results.
D	$(3+2n_w) \times n_a$	Matrix giving output quantities.
U	$(3+2n_w) \times 1$	Input column.
V	$n_a \times (3+2n_w)$	Input induced velocities.

—	Indicates peak amplitude.
[ ]	Indicates jump across blade of quantity inside brackets.
< >	Indicates time average.
$\mathscr{R}, \mathscr{I}$	Indicates real and imaginary parts.

Six of the elements of the matrix **C** will be referred to as follows,

$$\mathbf{C} = \begin{bmatrix} C_{Fq} & C_{F\alpha} & C_{Fw} & — & — & — \\ C_{Mq} & C_{M\alpha} & C_{Mw} & — & — & — \\ — & — & — & — & — & — \end{bmatrix}$$

LIST OF REFERENCES

No.	*Author(s)*	*Titles, etc.*
1	F. Lane and M. Friedman ..	Theoretical investigation of subsonic oscillating blade-row aerodynamics. N.A.C.A. Tech. Note 4136 (1958).
2	D. N. Gorelov and L. V. Dominas	Determination of unsteady aerodynamic forces for a space cascade of plates in a subsonic gas flow. *Mech. Zhid i Gaza, No.* 6 p. 21 (1967).
3	S. Kaji and T. Okazaki ..	Propagation of sound waves through a blade row. II. Analysis based on the acceleration potential method. *J. Sound Vib. Vol.* 11, p. 355 (1970).
4.	D. I. Blokhintsev	Acoustics of a non-homogeneous, moving medium. N.A.C.A. TM 1399 (1946).
5	F. P. Bretherton and C. J. R. Garrett	Wavetrains in inhomogeneous moving media. Proc. Roy. Soc. A 302, p. 529, (1968).
6	C. L. Morfey	Acoustic energy in non-uniform flows. *J. Sound Vib. Vol.* 14, p. 159 (1971).
7	J. M. Tyler and T. G. Sofrin ..	Axial flow compressor noise studies. Trans. S.A.E., Vol. 70, p. 309 (1962).
8	R. Mani	Discrete frequency noise generation from an axial flow fan blade row. Trans. A.S.M.E., D. Vol. 92, p. 37.
9	National Physical Laboratory	Modern Computing Methods. H.M.S.O., London (1961).
10	D. S. Whitehead	Force and Moment Coefficients for Vibrating Aerofoils in Cascade. ARC R. and M. 3254 (1960).
11	R. Parker	Resonance effects in wake shedding from parallel plates: calculation of resonant frequencies. *J. Sound Vib.*, Vol. 5, p. 330 (1967).
12	D. S. Whitehead	Bending Flutter of Unstalled Cascade Blades at Finite Deflection. ARC R. and M. 3386 (1962).
13	D. S. Whitehead	Torsional Flutter of Unstalled Cascade Blades at Zero Deflection. ARC R. and M. 3429 (1964).

TABLE 1

Comparison with Incompressible Results.

Frequency Parameter = 2·0

Mach No. = 0

Space/Chord = 1·0

n_a = 4

$\xi = 0 \quad \sigma/2\pi = 0{\cdot}5$

	Bending		Torsion		Wakes	
C_F	−0·7303	−0·3820	−0·4384	−1·4372	−0·3245	+0·3743
	−0·7318	−0·3817	−0·4409	−1·4382	−0·3249	+0·3752
C_M	−0·2026	−0·2363	+0·0408	−0·6594	−0·0900	+0·1038
	−0·2035	−0·2362	+0·0395	−0·6602	−0·0903	+0·1043

$\xi = 45° \quad \sigma/2\pi = 0{\cdot}5$

	Bending		Torsion		Wakes	
C_F	−0·6840	−0·3160	−0·4673	−1·3036	−0·2680	+0·3548
	−0·6796	−0·3180	−0·4596	−1·3020	−0·2671	+0·3518
C_M	−0·1903	−0·2073	+0·0197	−0·6015	−0·0745	+0·0988
	−0·1875	−0·2080	+0·0239	−0·5998	−0·0737	+0·0971

$\xi = 75° \quad \sigma/2\pi = 0{\cdot}8$

	Bending		Torsion		Wakes	
C_F	−0·2841	−0·3792	+0·0309	−0·7971	−0·2806	0·0116
	−0·2686	−0·3821	+0·0428	−0·7822	−0·2741	−0·0064
C_M	−0·0757	−0·2210	+0·1598	−0·4561	−0·0710	0·0066
	−0·0685	−0·2264	+0·1658	−0·4573	−0·0661	−0·0050

Notes—For each coefficient first the real part and then the imaginary part is shown on the same line.

The first line gives the result from the present program. The second line gives the result from Ref. 10. These coefficients are referred to an axis position at the *leading edge.*

TABLE 2

Comparison with Lane and Friedman.

Space/Chord = 3·8

Stagger = 0

$\sigma/2\pi$ = 0·5

Mach No. = 0·5

n_a = 3

Frequency Parameter = 1·0

	Bending		Torsion	
C_F	−0·7212	+0·0665	−0·8277	−0·0866
	−0·7200	+0·0672	−0·8266	−0·0856
C_M	+0·1509	−0·1051	+0·1826	−0·1496
	+0·1506	−0·1052	+0·1824	−0·1497

Frequency Parameter = 1·2

	Bending		Torsion	
C_F	−0·7546	+0·0962	−0·9137	−0·0660
	−0·7538	+0·0959	−0·9127	−0·0664
C_M	+0·1323	−0·1301	+0·1733	−0·1964
	+0·1323	−0·1300	+0·1733	−0·1961

Frequency Parameter = 1·4

	Bending		Torsion	
C_F	−0·3383	+0·4648	−0·5077	+0·5073
	−0·3433	+0·4670	−0·5158	+0·5077
C_M	−0·0303	−0·1167	−0·0319	−0·2319
	−0·0306	−0·1180	−0·0310	−0·2344

Notes—For each coefficient first the real part and then the imaginary part is shown on the same line. The first line gives the result from the present program. The second line gives the result from Ref. 1. These coefficients are referred to an axis position at the *mid-chord point.*

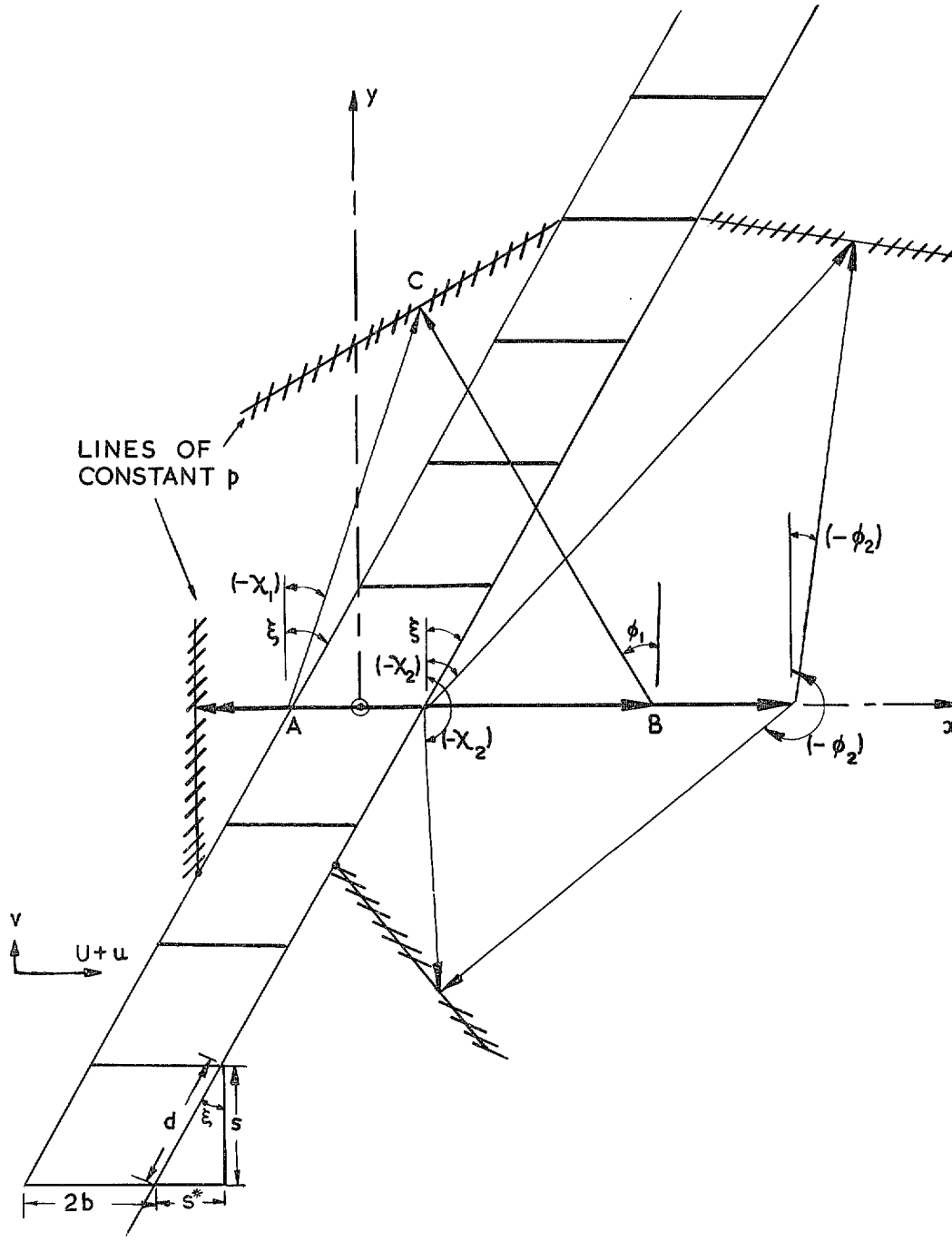

FIG. 1. Physical plane drawn for
$\frac{d}{2b} = 1, \xi = 30°, \frac{\sigma}{2\pi} = \frac{3}{4}, M = 0{\cdot}8, 2k = \frac{3\pi}{4}$.

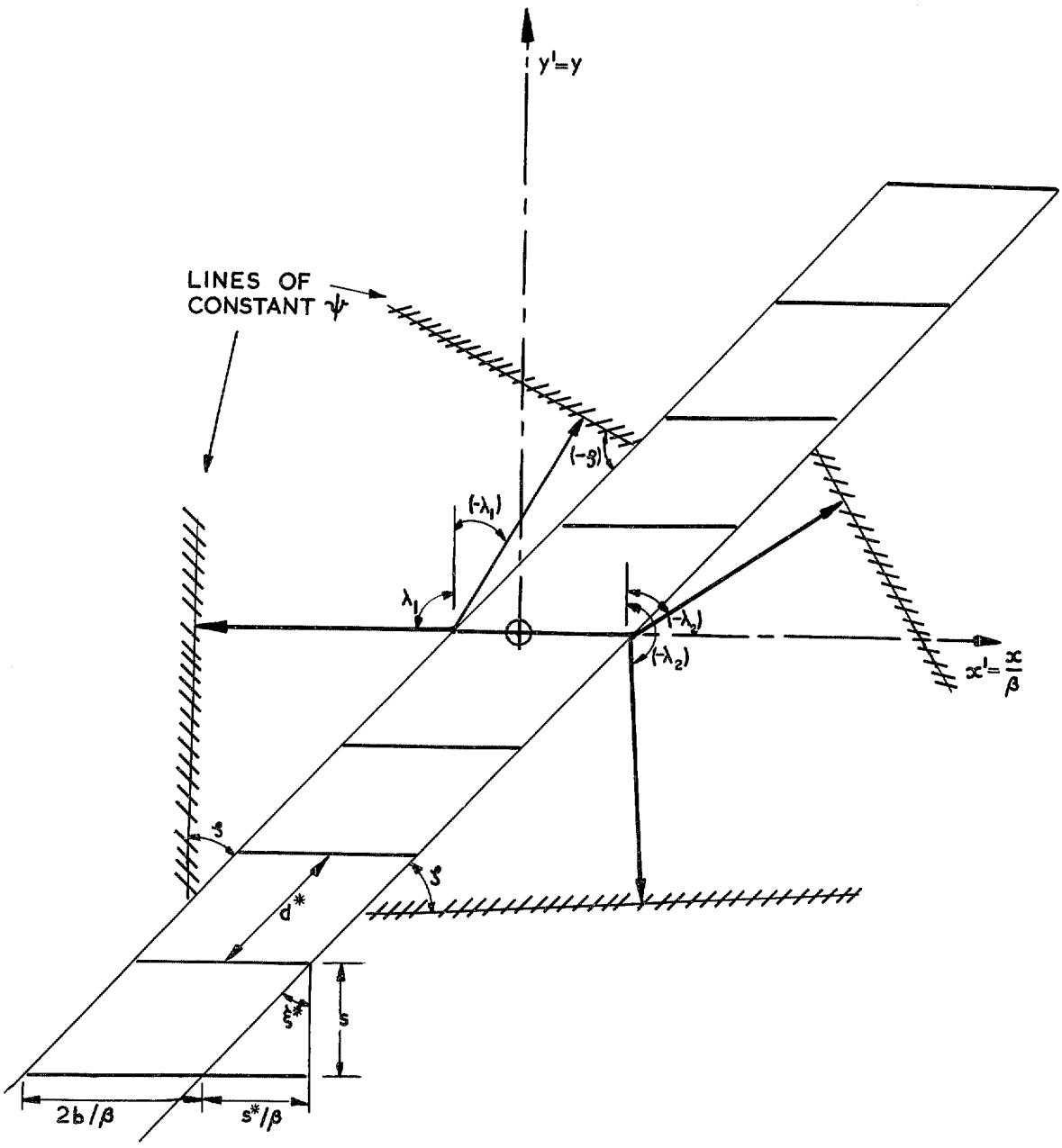

FIG. 2. Prandtl-Glauert plane drawn for $\frac{d}{2b} = 1, \xi = 30°, \frac{\sigma}{2\pi} = \frac{3}{4}, M = 0{\cdot}8, 2k = \frac{3\pi}{4}$.

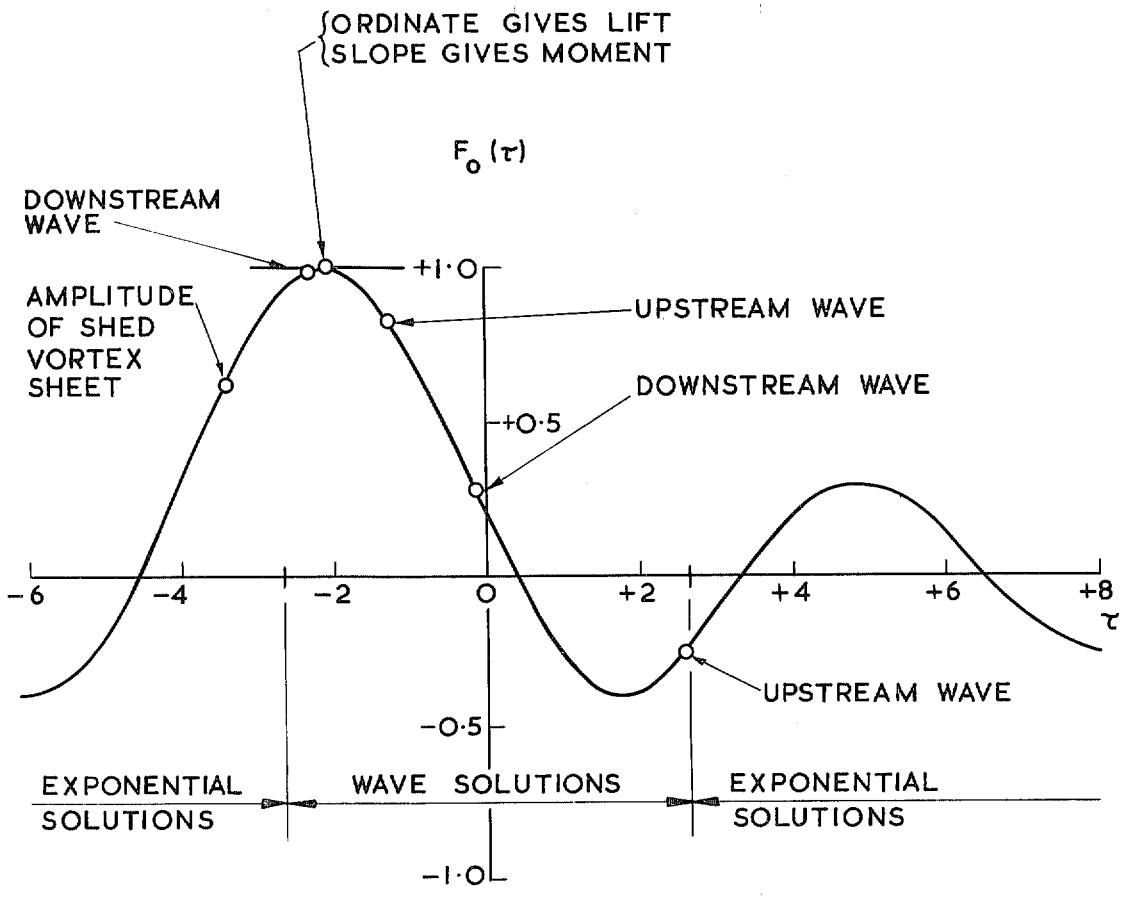

FIG. 3. Example of $F_o(\tau)$ function drawn for $\left(\frac{d}{2b}\right) = 1, \xi = 30°, \frac{\sigma}{2\pi} = \frac{3}{4}, M = 0{\cdot}8, 2k = \frac{3\pi}{4}$.

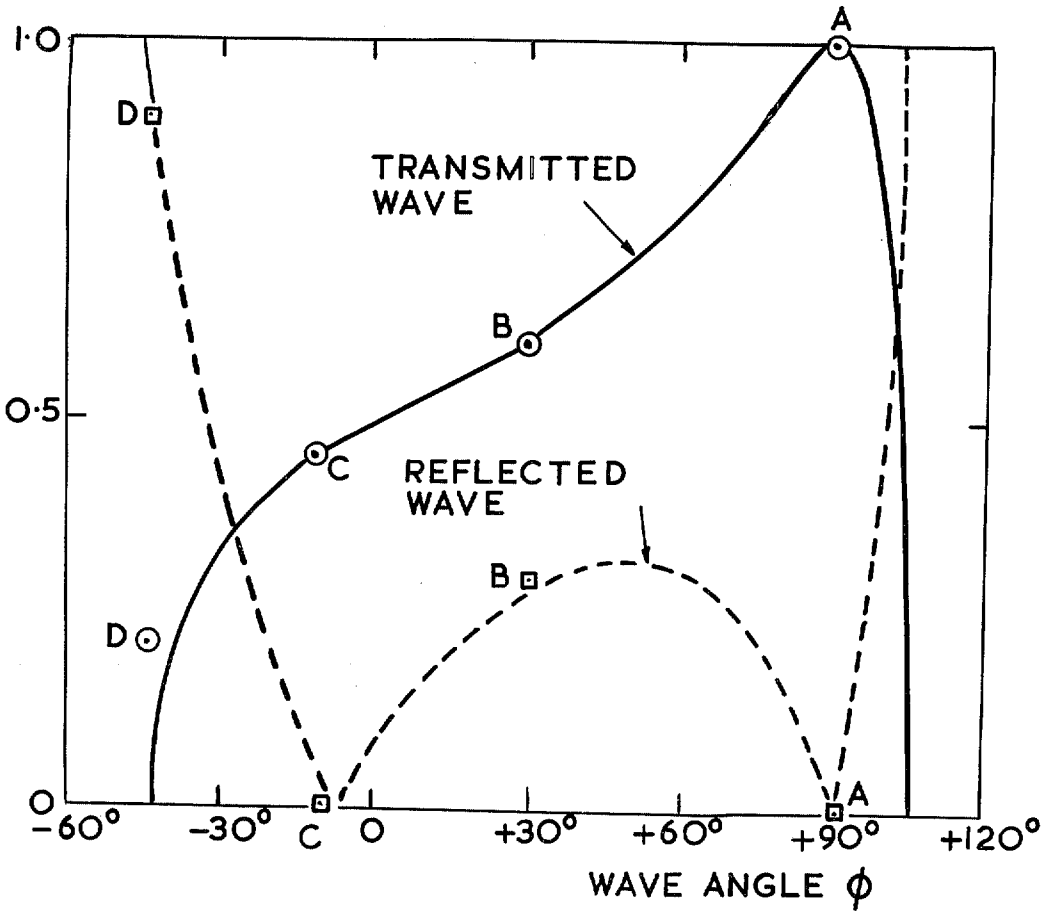

FIG. 4. Comparison with Kaji and Okazaki.
$\frac{d}{2b} = 1, \xi = 60°, M = 0{\cdot}5, 2k = \frac{\pi}{2}$.

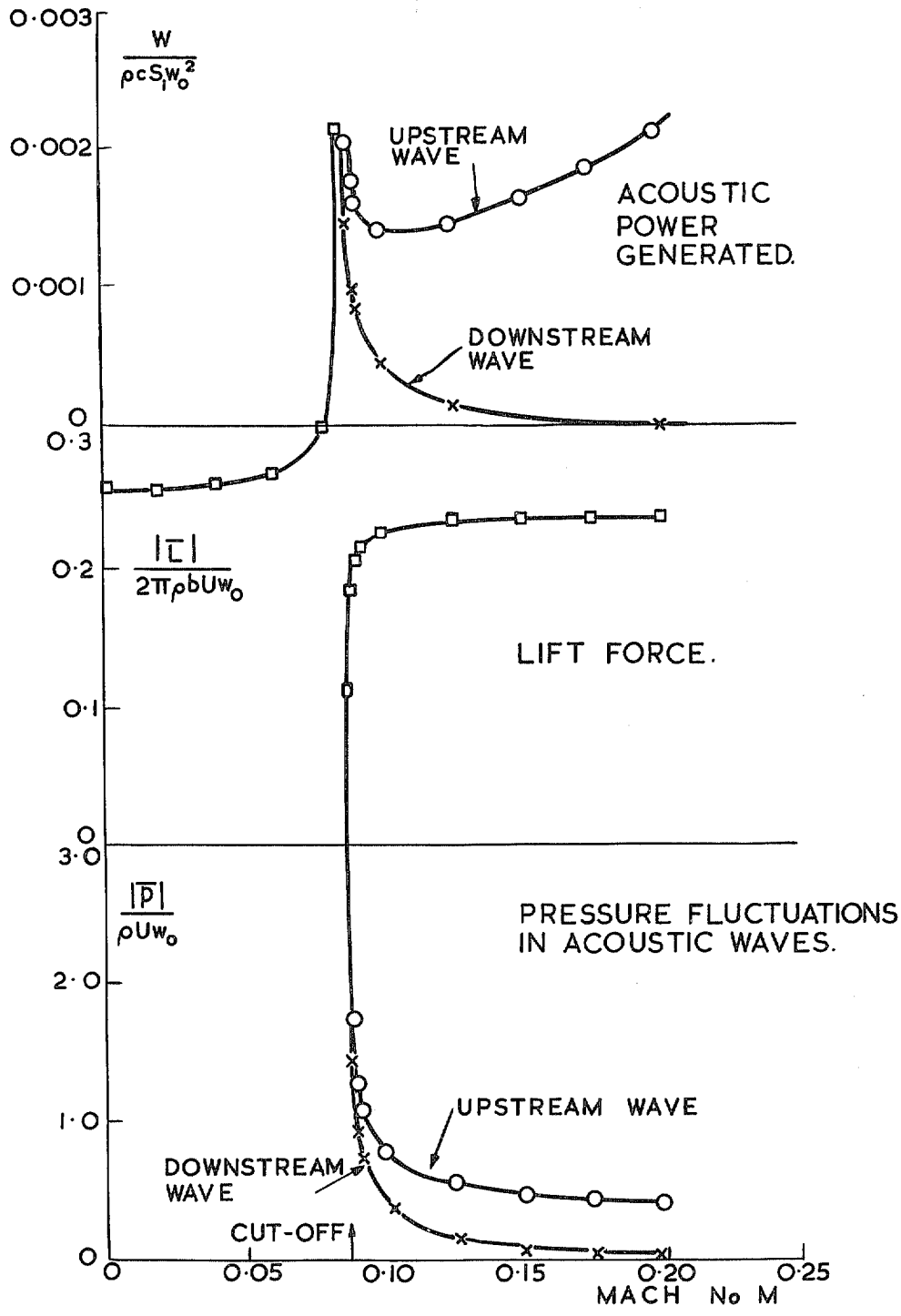

FIG. 5. Lift and acoustic wave generation by wakes
$\frac{d}{2b} = 0{\cdot}955, \xi = 30°, 2k = 3{\cdot}435, \frac{\sigma}{2\pi} = -\frac{24}{23}$.

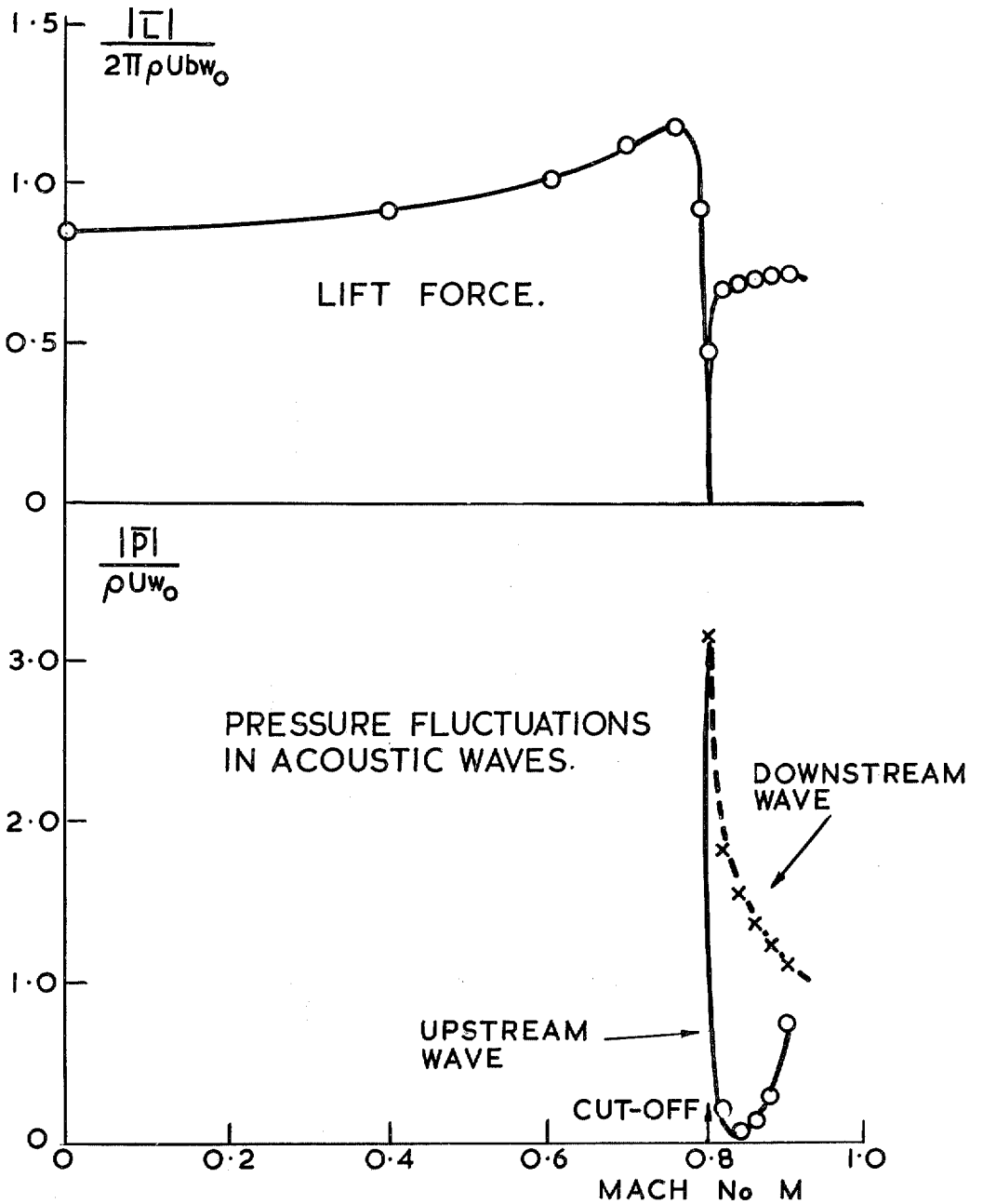

FIG. 6. Lift and acoustic wave generation at high Mach No.
$\frac{d}{2b} = 1, \xi = 30°, 2k = 0{\cdot}631, \frac{\sigma}{2\pi} = \frac{1}{4}$.

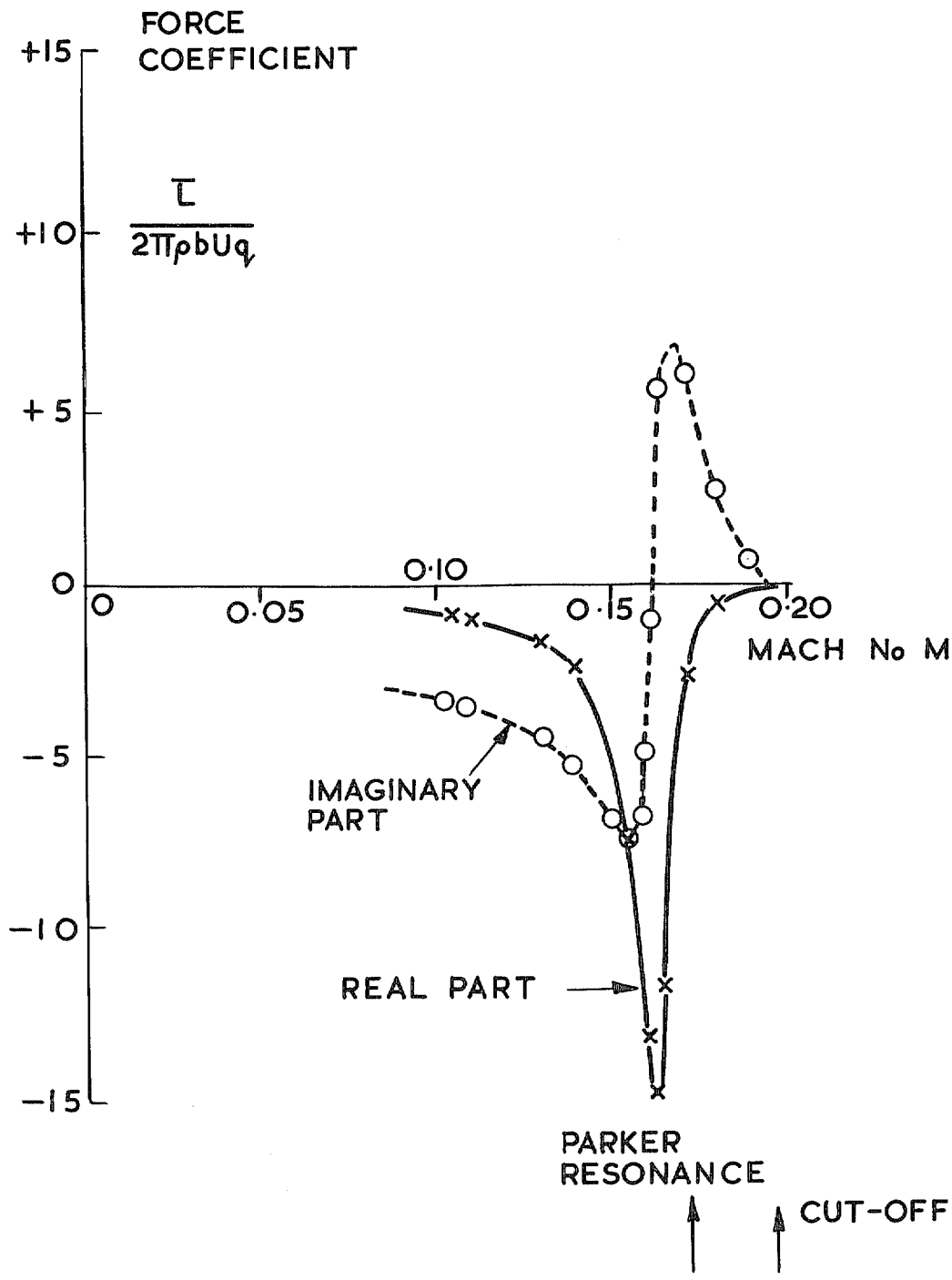

FIG. 7. Comparison with Parker's resonance.
$\frac{d}{2b} = 1{\cdot}59, \xi = 0, 2k = 10, \frac{\sigma}{2\pi} = 0{\cdot}5$.

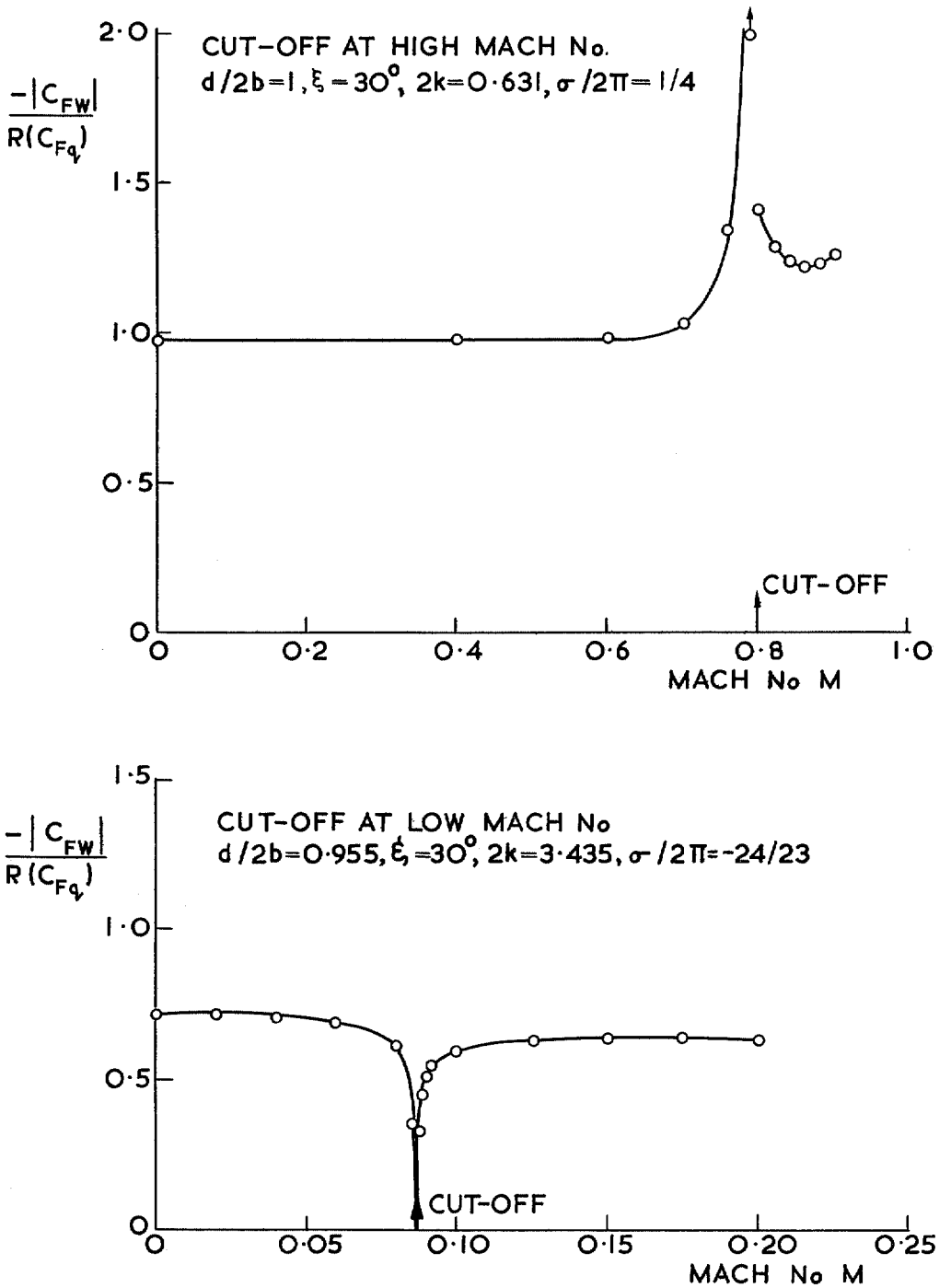

FIG. 8. Resonance factors for bending Vibration.

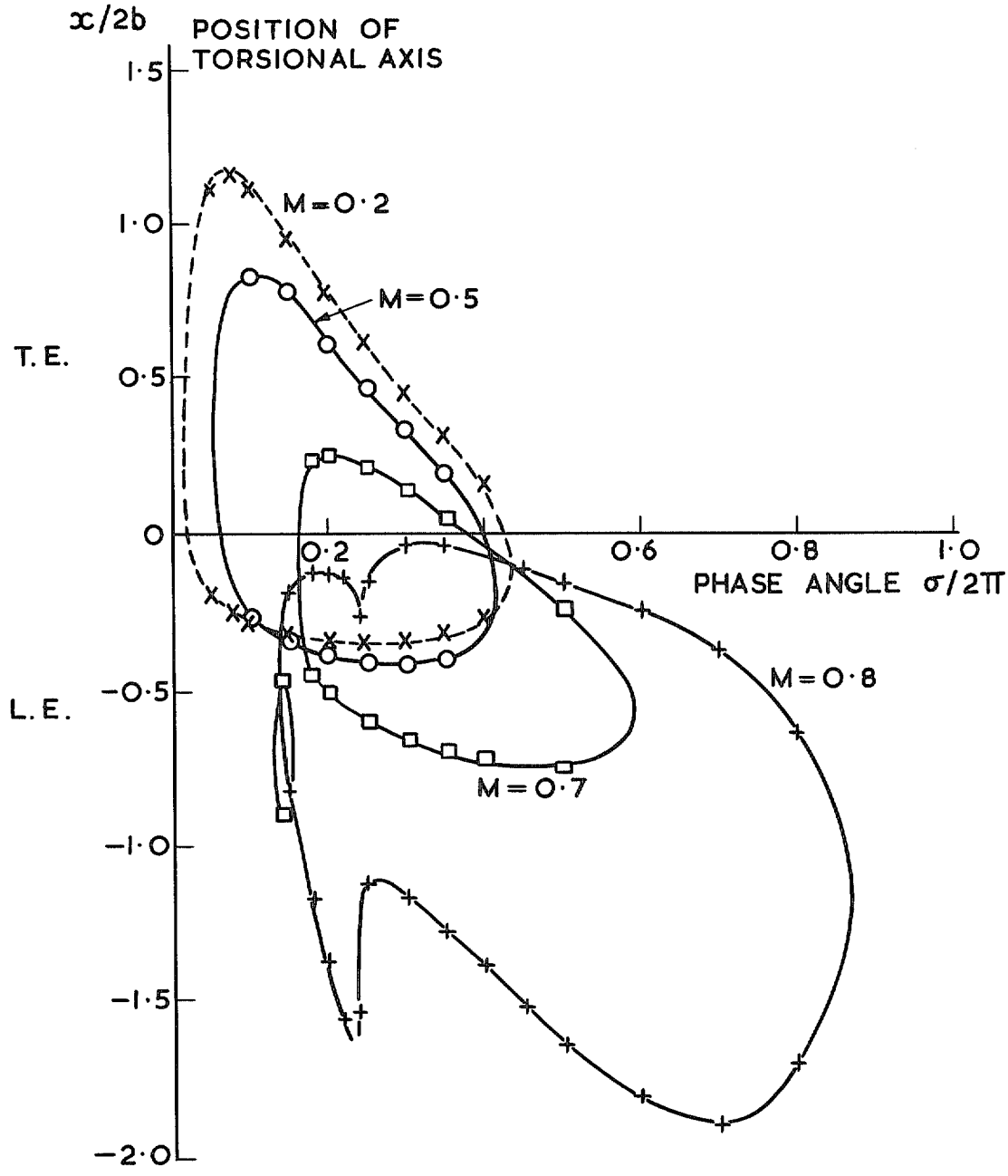

FIG. 9. Torsional flutter.
$\frac{d}{2b} = 0{\cdot}8, \xi = 65°, 2k = 0{\cdot}5$.

Printed in Wales for Her Majesty's Stationery Office by Allens Printers (Wales) Limited
Dd. 502110 K.5.

Published by
HER MAJESTY'S STATIONERY OFFICE

To be purchased from
49 High Holborn, London WC1V 6HB
13a Castle Street, Edinburgh EH2 3AR
109 St Mary Street, Cardiff CF1 1JW
Brazennose Street, Manchester M60 8AS
50 Fairfax Street, Bristol BS1 3DE
258 Broad Street, Birmingham B1 2HE
80 Chichester Street, Belfast BT1 4JY
or through booksellers

R. & M. No. 3685

SBN 11 470485 6